

Free Majorana Fermion Meets Gauged Ising Conformal Field Theory on the Fuzzy Sphere

Zheng Zhou (周正),^{1,2} Davide Gaiotto,¹ and Yin-Chen He³

¹*Perimeter Institute for Theoretical Physics, Waterloo, Ontario N2L 2Y5, Canada*

²*Department of Physics and Astronomy, University of Waterloo, Waterloo, Ontario N2L 3G1, Canada*

³*C. N. Yang Institute for Theoretical Physics, Stony Brook University, Stony Brook, NY 11794-3840*

11th September 2025

ABSTRACT: The fuzzy sphere regularisation is a powerful tool to study conformal field theories (CFT) in three spacetime dimensions. In this paper, we extend its scope to CFTs with local fermionic operators. We realise the free Majorana fermion CFT on a setup with one flavour of bosons and one flavour of fermions on the lowest Landau level with a 1/2 angular momentum mismatch. We allow conversion between two bosons and two fermions, and use a relative chemical potential as the tuning parameter. On the phase diagram, we find three gapped phases, *viz.* a fermionic integer quantum Hall phase, an f -wave chiral topological superconductor, and a bosonic Pfaffian phase. They are separated by two continuous transitions described respectively by a free Majorana fermion and a gauged Ising CFT. We numerically confirm their emergent conformal symmetry through the operator spectrum. We also study the two-point correlation function of the Majorana fermion, and the topological Wilson line defect of the gauged Ising CFT. Our work lays the foundation for studying interacting fermionic CFTs and regularising quantum field theories on the fuzzy sphere.

Contents

| | | |
|----------|--|-----------|
| 1 | Introduction | 1 |
| 2 | Model | 5 |
| 3 | Phase Diagram | 8 |
| 4 | Critical Theories | 12 |
| 5 | Free Majorana Fermion CFT | 15 |
| 6 | Gauged Ising CFT | 19 |
| 7 | Discussion | 22 |
| A | Edge CFT Character and Entanglement Spectrum Degeneracy Count | 26 |
| B | Lagrangian Description of the Gauged Ising Transition | 28 |
| C | Realisation of Local Spinor Operators on the Fuzzy Sphere | 29 |
| | Bibliography | 33 |

1 Introduction

Conformal field theory (CFT) is one of the central topics of modern physics. CFT has provided important insights into various aspects of theoretical physics. In condensed matter physics, it has produced useful predictions about the critical phenomena [1–3]. Many classical and quantum phase transitions are conjectured to have emergent conformal symmetry in the infrared (IR). In high energy physics and quantum field theories, CFT also plays important role in understanding string theory [4], duality with gravitational theories on anti-de Sitter (AdS) space [5], and renormalisation group flow structure [6]. In 2D, the infinite-dimensional conformal algebra has made many theories exactly solvable [7–9]. However, going to the higher dimensions, the CFTs are less well-studied due to a much smaller conformal group. Some of the conformal data are determined at high precision by conformal bootstrap [10, 11].

Fermionic CFTs, *i.e.* CFTs that include fermionic local operators, constitute a particularly interesting type of CFTs, including Gross-Neveu-Yukawa theories and certain gauge theories with or without Chern-Simons (CS) term. In some special cases, these CFTs can have emergent supersymmetry. For example, the theory of a single Majorana fermion coupled to a real Yukawa scalar field flows to a superconformal field theory with $\mathcal{N} = 1$ in the IR, known as the super-Ising theory [12–14]. Experimentally, these fermionic CFTs are easier to detect than their bosonic counterparts, as they produce rich electric signals, to which most experimental probes are naturally sensitive. For example, the frequency dependence of conductivity can be measured through electric transport experiments, and it corresponds to the OPE of the conserved symmetry current $J \times J$ [15, 16], including the central charge C_J from its two-point function. An outstanding platform is the Moiré materials [17–19]. Through tuning many available knobs like potential amplitude, they can be used to realise plateau transitions between fractional Chern insulators [20–22]. However, the nature and critical data of these theories remain poorly understood.

The fuzzy sphere regularisation [23] has emerged as a new powerful method to study 3D CFTs. This method involves studying quantum systems on a sphere that is ‘fuzzy’ (non-commutative) due to a magnetic monopole at its centre. It offers distinct advantages including the exact preservation of rotation symmetry, the direct observation of emergent conformal

symmetry and the efficient extraction of conformal data. In the fuzzy sphere method, the state-operator correspondence plays an essential role. Specifically, there is a one-to-one correspondence between the eigenstates of the critical Hamiltonian on the sphere and the CFT operators, where the energy gaps are proportional to the scaling dimensions. The power of this approach has been first demonstrated in the context of the 3D Ising transition [23], where the presence of emergent conformal symmetry has been convincingly established. Since its proposal, various studies have greatly expanded its horizon [23–50], including

1. accessing the ‘conformal data’ of the 3D Ising CFT such as the OPE coefficients [24, 42], correlation functions [25], entropic F -function [31], conformal generators [36, 37] and crosscap coefficients [50],
2. studying the conformal defects, boundaries such as the magnetic line defect [27], its g -function and defect changing operators [30], its cusp [32], and various conformal boundaries in the 3D Ising CFT [33, 35],
3. realising various 3D CFTs such as the Wilson-Fisher CFTs [29], $SO(5)$ [26] and $O(4)$ [48] deconfined criticality, a series of new $Sp(N)$ CFTs [38], Potts model [40], Yang-Lee criticality [43–45], free real scalar [46, 47] and Chern-Simons-matter CFTs [49].

All the CFTs that have been realised on fuzzy sphere so far have purely bosonic operator content. Apart from the fuzzy sphere regularisation, a recent exploratory attempt to access the fermionic Gross-Neveu-Yukawa CFT considered Dirac fermions on a conventional sphere, using a basis of spinor spherical harmonics [51]. Although intuitive, this approach suffers from UV divergences similar to those in standard QFTs on continuous space, and thus further theoretical and numerical efforts may be required to justify its validity. In contrast, the fuzzy sphere approach, similar to the highly successful lattice regularisation of QFTs and strongly interacting condensed matter lattice models, is free of UV divergences [46].¹ Consequently, the study of fermionic CFTs would greatly benefit from a fuzzy sphere realisation, especially in light of the success achieved for their bosonic counterparts.

Nevertheless, the fuzzy sphere realisation of fermionic CFTs faces some challenges. Most

¹In the continuum limit (*i.e.* the monopole flux $q \rightarrow \infty$) of the fuzzy sphere model, any (bare) local operator, as well as its correlators, remain non-diverging. Moreover, the microscopic couplings at the critical point also remain finite, *i.e.*, they converge to finite values in the continuum limit.

fuzzy sphere models are built of microscopic fermions, *i. e.* the fermions with U(1) electric charge on the lowest Landau level. These microscopic fermions experience the magnetic field generated by the monopole and thus become fuzzy, in the sense that they have strong non-commutativity inherited from the magnetic field. For example, in flat space the microscopic fermions transform in a *projective* representation of the continuous translation group, which is incompatible with any local operator of a CFT. The resolution is that these microscopic fermions must be gapped, so that the electric charge U(1) is decoupled from the IR critical theory. Gapless ‘local’ CFT operators on the fuzzy sphere tend to involve bilinear expressions in the microscopic fermions, which are charge neutral and bosonic. Moreover, another challenge is that the fermionic field in the CFT should carry half-integer spin (angular momentum), a requirement that microscopic fermions may not automatically satisfy. In this paper, we show that these challenges can be overcome by a fuzzy sphere model with boson-fermion mixture. Concretely, we consider a setup with both microscopic bosons b and fermions f with the same electric charge and let their angular momenta differ by 1/2. Their bilinears $b^\dagger f$ or $f^\dagger b$ are neutral under electric charge and have fermionic statistics as well as half-integer spins. Therefore, the bilinears can be used to realise fermionic local operators in a CFTs.²

The simplest fermionic CFT to target is the free Majorana fermion CFT. Its Lagrangian is

$$\mathcal{L}_{\text{Majorana}} = \frac{1}{2} \bar{\chi} (i \not{\partial} - m) \chi, \quad (1.1)$$

where χ is a two component spinor, $\bar{\chi} = \chi^T \epsilon$, $\epsilon = i \sigma^2$, and $\not{\partial} = \sigma^\mu \partial_\mu$. The free Majorana fermion χ has exact scaling dimension $\Delta_\chi = 1$ and is subject to the equation of motion $\not{\partial} \chi = 0$.³ It describes a transition driven by the mass m . Masses with different signs flow respectively to a trivially gapped phase and a p -wave chiral topological superconductor [52, 53] (TSC), which is a gapped phase characterised by a parity and time-reversal breaking fermion pairing, thermal Hall conductance or chiral central charge $c_- = 1/2$ and a chiral free Majorana fermion mode

²A recent work [49] have also studied a boson-fermion mixture fuzzy sphere model that realises the confinement transition of $\nu = 1/2$ bosonic Laughlin state. Its setup involves two flavours of charge-1 microscopic fermions and a flavour of charge-2 microscopic bosons. Hence, the charge-0 CFT operators are still bosonic.

³Unitarity and conformal symmetry imply that any local operator of spin- $\frac{1}{2}$ with $\Delta = 1$ is a free fermion, so this scaling dimension also gives a clear criterion to identify the free fermion CFT.

on the edge.⁴

In this paper, we study the setup with one flavour of fermions and one flavour of bosons on the fuzzy sphere with the same electric charge but a mismatch $1/2$ in the angular momenta. We set the total filling $\nu = 1$ and allow the conversion between two fermions and two bosons. By tuning a relative chemical potential, we identify a fermionic integer quantum Hall (fIQH) phase at $\nu_f = 1$ when fermions are energetically favourable, a bosonic Pfaffian (bPf) phase [52, 54] at $\nu_b = 1$ with topological order characterised by a $SU(2)_2$ Chern-Simons theory when bosons are energetically favourable, and an intermediate gapped phase corresponding to an f -wave TSC (*i.e.* a p -wave TSC on the background of a $\nu_f = 1$ fIQH state). We show theoretically and numerically that the fIQH-TSC transition is described by a free Majorana fermion CFT. In particular, the energy gap, operator spectrum and two-point correlation function of local fermion all agree well with the free Majorana fermion CFT.

On the other hand, the TSC-bPf transition is described by an Ising CFT coupled to a \mathbb{Z}_2 gauge field. The gauged Ising universality, also known as Ising*, was first studied in the confinement transition of \mathbb{Z}_2 topological order [55–61]. While the Ising* criticality was first proposed to describe the transition between a trivially gapped state and a \mathbb{Z}_2 topological order, in our setup, confining a \mathbb{Z}_2 gauge field drives the bPf phase to an TSC with trivial topological order. The only difference is a TSC background that does not change the universality. This is numerically confirmed by the agreement of the operators spectrum with the \mathbb{Z}_2 -even sector of the Ising CFT. An interesting feature of the gauged Ising CFT is the topological Wilson line defect. We show that a \mathbb{Z}_2 gauge charge as the endpoint of the Wilson line can be inserted by inserting a 2π monopole flux, and the endpoint operators correspond to the \mathbb{Z}_2 -odd sector of the Ising CFT.

In short, our boson-fermion mixture construction successfully extends the fuzzy sphere approach to fermionic CFTs, opening avenues to explore a broad class of theories, including the Gross-Neveu-Yukawa, super-Ising, and quantum Hall transitions relevant to Moiré materials. A key ingredient is to create a half-integer fermionic field through the angular momentum offset of $1/2$ between microscopic fermions and bosons. This idea might be generalisable to define

⁴Albeit the name ‘superconductor,’ the TSC do not spontaneously break any $U(1)$ symmetry.

CFTs such that the most relevant operators have non-trivial spin: a ‘pure symmetry’ CFT such that the simplest local operators are conserved currents of spin-1, or a ‘pure energy’ CFT such that the simplest local operator is the stress tensor, a property expected from holographic duals to theories of quantum gravity [62–64]. Both would be examples of ‘self-organised’ critical theories stable to any deformation. It may also give a route to engineer spin-1 gauge fields and thus implement general renormalisable Lagrangians of quantum field theories on the fuzzy sphere. It may also be possible to reach effective field theories with higher spin quantum fields. The realisation of the gauged Ising CFT provides new possibilities in studying line defects like monodromy defect in Ising CFT. Last but not least, we remark that the entire phase diagram of our model, including the three gapped phases and two critical points, can be captured by a single Lagrangian of adjoint QCD [65]. A natural future direction is to explore whether a similar setup can be used to study other gauge theories that exhibit rich phase diagrams as well as novel interacting CFTs.

This paper is organised as the following: In Section 2, we present the setup of fuzzy sphere and our model Hamiltonian. In Section 3, we present the phase diagram supported by the numerical evidences for the gapped phases. In Section 4, we analyse the critical theories that describe the two continuous transitions between the three gapped phases. Then, Sections 5 and 6 are devoted to the numerical results respectively for the free Majorana fermion CFT and the gauged Ising CFT. Finally, in Section 7, we make a brief summary and discuss the implications of our work and future directions.

2 Model

In the setup of the fuzzy sphere [66], we consider one flavour of fermions f and one flavour of bosons b with the same electric charge on the sphere under the influence of a magnetic monopole at its centre. We let the monopole charge they experience differ by 2π , *i.e.*, we let the fermion experience a $4\pi q$ monopole and the bosons experience a $4\pi(q - \frac{1}{2})$ monopole. As will be elaborated below, the mismatch of the monopole flux reflects the coupling between the electric charge and the spatial curvature, and it also allows the fermionic local operators like $f^\dagger b$ to have half-integer angular momenta. Due to the presence of the monopole, the single-

particle eigenstates form highly degenerate quantised Landau levels [67]. The lowest Landau level (LLL) has angular momentum q and degeneracy $N_{mf} = 2q + 1$ for the fermions and angular momentum $q - \frac{1}{2}$ and degeneracy $N_{mb} = 2q$ for the bosons. By setting the single particle gap the leading energy scale, we project the system onto the LLL and express the fermion and boson operators in terms of the creation and annihilation operators on the LLL

$$f^\dagger(\mathbf{r}) = \frac{1}{R} \sum_{m=-q}^q f_m^\dagger Y_{qm}^{(q)}(\mathbf{r}), \quad b^\dagger(\mathbf{r}) = \frac{1}{R} \sum_{m=-q+1/2}^{q-1/2} b_m^\dagger Y_{q-1/2,m}^{(q-1/2)}(\mathbf{r}), \quad (2.1)$$

where the radius of the sphere is set as $R = N_{mf}^{1/2}$ [23], and the single particle wavefunctions are the spin-weighted spherical harmonics [68].

The symmetries we preserve are:

1. A $U(1)_e$ corresponding to the conservation of total electric charge $N_e = N_b + N_f$. This symmetry decouples from the low energy dynamics at the critical points, but it can still lead to non-trivial topological effect (*cf.* Section 6). We set $N_e = N_{mf}$ and allow the conversion between bosons and fermions.
2. The $SU(2)$ sphere rotation symmetry. The spatial parity is not manifest in our model, which frees us from the constraint of parity anomaly in theories like single free Majorana fermion. The conservation of fermion parity, whose charge is $(-1)^{N_f}$, is a part of this rotation symmetry. Because the boson and fermion orbitals have an angular momentum mismatch of $1/2$, the fermion parity even states have integer spin under $SU(2)$ and the fermion parity odd states have half-integer spin under $SU(2)$. In other words, we are building in spin-statistics rather than having it emerge in the relativistic IR CFT.

The Hamiltonian we study includes the simplest symmetry-allowed terms:

1. The local electric charge density interaction $H_U = \int d^2\mathbf{r} (n_f(\mathbf{r}) + n_b(\mathbf{r}))^2$, where $n_f(\mathbf{r}) = f^\dagger(\mathbf{r})f(\mathbf{r})$, $n_b(\mathbf{r}) = b^\dagger(\mathbf{r})b(\mathbf{r})$. This term is a natural form of interaction that exists in many other fuzzy sphere models (*e.g.* Refs. [23, 26, 46, 49]).
2. A local boson-fermion pair conversion H_t which annihilates two fermions and creates two bosons or vice versa. This term breaks the separate conservation of boson and fermion numbers to the total electric charge conservation. The conversion must occur in pair to preserve the fermion parity.

3. A relative chemical potential μN_f , which enables us to energetically favour bosons or fermions.

Altogether,

$$\begin{aligned}
H &= H_U + tH_t + \mu N_f \\
H_U &= \int d^2\mathbf{r} (n_f(\mathbf{r}) + n_b(\mathbf{r}))^2 \\
&= \sum_{\{m_i\}} M_{m_1 m_2 m_3 m_4}^{(b)} b_{m_1}^\dagger b_{m_2}^\dagger b_{m_3} b_{m_4} + M_{m_1 m_2 m_3 m_4}^{(bf)} b_{m_1}^\dagger f_{m_2}^\dagger f_{m_3} b_{m_4} \\
H_t &= \sum_{\{m_i\}} M_{m_1 m_2 m_3 m_4}^{(t)} b_{m_1}^\dagger b_{m_2}^\dagger f_{m_3} f_{m_4} + \text{h.c.}
\end{aligned} \tag{2.2}$$

The four-fermion contact terms are equivalently expressed in terms of the pseudopotentials [23, 67]

$$\begin{aligned}
M_{m_1 m_2 m_3 m_4}^{(t)} &= \frac{\delta_{m_1+m_2, m_3+m_4}}{2q-1} \begin{pmatrix} q - \frac{1}{2} & q - \frac{1}{2} & 2q-1 \\ m_2 & m_1 & -m_1 - m_2 \end{pmatrix} \begin{pmatrix} q & q & 2q-1 \\ m_3 & m_4 & -m_3 - m_4 \end{pmatrix} \\
M_{m_1 m_2 m_3 m_4}^{(b)} &= \frac{\delta_{m_1+m_2, m_3+m_4}}{2q-1} \begin{pmatrix} q - \frac{1}{2} & q - \frac{1}{2} & 2q-1 \\ m_2 & m_1 & -m_1 - m_2 \end{pmatrix} \begin{pmatrix} q - \frac{1}{2} & q - \frac{1}{2} & 2q-1 \\ m_3 & m_4 & -m_3 - m_4 \end{pmatrix} \\
M_{m_1 m_2 m_3 m_4}^{(bf)} &= \frac{\delta_{m_1+m_2, m_3+m_4}}{2q - \frac{1}{2}} \begin{pmatrix} q & q - \frac{1}{2} & 2q - \frac{1}{2} \\ m_2 & m_1 & -m_1 - m_2 \end{pmatrix} \begin{pmatrix} q & q - \frac{1}{2} & 2q - \frac{1}{2} \\ m_3 & m_4 & -m_3 - m_4 \end{pmatrix}.
\end{aligned}$$

where $(\bullet\bullet\bullet)$ is the Wigner's $3j$ -symbol. Note that in H_t , the orbital indices of the two bosons are symmetrised and fermions are antisymmetrised. In real space, the pair conversion is equivalent to

$$H_t = \int d^2\mathbf{r} (b^\dagger f)(\mathbf{r}) (D_\theta + iD_\phi) (b^\dagger f)(\mathbf{r}) + \text{h.c.} \tag{2.3}$$

where D^μ is the covariant derivative on the sphere.⁵ Interestingly, this pair conversion can be understood as a kinetic term of the Majorana fermion (*cf.* Section 5).

Let us consider some limiting cases for μ . At large negative μ , fermions are energetically favourable and the fermion orbitals are fully filled, forming a fermionic integer quantum Hall (fIQH) state with $\nu_f = 1$. At large positive μ , bosons are energetically favourable, and the boson density interaction drives a bosonic Pfaffian (bPf) state [54, 69]. The mismatch of number of

⁵Specifically, $D^\mu = \partial^\mu + iqA^\mu$, where $b^\dagger f$ experiences a monopole flux $q = -1/2$, and $A^\phi = \text{ctg } \theta$

orbitals and particles $N_e = N_{mb} + 1$ is in agreement with the Wen-Zee shift required by the bPf state [70, 71] which arises from the coupling between the electric charge and the spatial curvature. We will discuss this phase in more detail in Section 3.

3 Phase Diagram

We study this model numerically through exact diagonalisation (ED) using our numerical package FuzzifiedED [72].⁶ The maximal system size we reach is $N_{mf} = 13$, and the maximal RAM usage is 24 gigabytes. We first study the phase diagram on the t - μ plane. For finite t , we find that the fermion density drops continuously from 1 to 0 with increasing μ (Figure 1).⁷

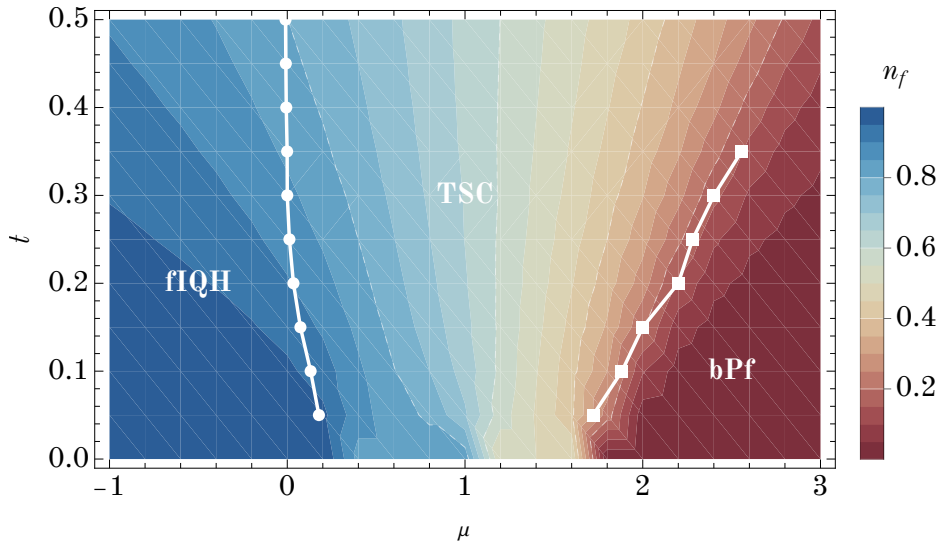


Figure 1. The phase diagram on the μ - t plane. The colour denotes the average fermion density calculated at $N_{mf} = 12$. Selected contours are marked by dashed lines as visual guidance. The circles separate the fermionic integer quantum Hall (fIQH) phase and the f -wave chiral topological superconductor (TSC), and the squares separate TSC and bosonic Pfaffian (bPf) phase. The approximate phase boundary is determined through the scaling of the energy gap from $N_{mf} = 12$ and 10 data.

⁶The module Fuzzifino, which is part of FuzzifiedED, specialises in the ED for boson-fermion mixed systems. Sample codes can be found at [FuzzifiedED.jl/examples/free_majorana_spectrum.jl](#) and [free_majorana_correlator.jl](#).

⁷For $t = 0$, the number of fermions and bosons are separately conserved, level crossings appear for states in different N_f sectors. The positive and negative t 's give exactly the same results, as they are connected by a 2π -rotation along z axis.

To study the nature of the fIQH-bPf transition, we first fix $t = 0.3$. We calculate the finite size behaviour of the fermionic gap ΔE_f , defined as the energy difference between the lowest excited state with angular momentum $l = 1/2$ and the ground state at $l = 0$, and the bosonic gap ΔE_b defined as the energy difference between the two lowest $l = 0$ states. At a Lorentz-invariant critical point, the gap is supposed to close as $\Delta E \propto 1/R$. We find two such critical points. At $\mu_{c1} \approx 0$, both bosonic and fermionic gap close; at $\mu_{c2} \approx 2.3$, the bosonic gap closes while the fermionic gap remains (Figure 2). We keep the data only for even N_{mf} near μ_{c2} because the bPf ground state is only compatible with even N_{mf} ; for odd N_{mf} , the phase and the transition still exist, but the states have an anyon excitation (cf. Section 6). Similar scenario holds for other finite t . For each t , we determine the approximate phase boundary by comparing the energy gaps for $N_{mf,1} = 12$ and $N_{mf,2} = 10$ (Figure 1): We minimise $[\Delta E(N_{mf,1})/\Delta E(N_{mf,2})](N_{mf,1}/N_{mf,2})^{1/2}$ respectively for the fermion gap and for the boson gap to get μ_{c1} and μ_{c2} . The minima are typically value close to 1.

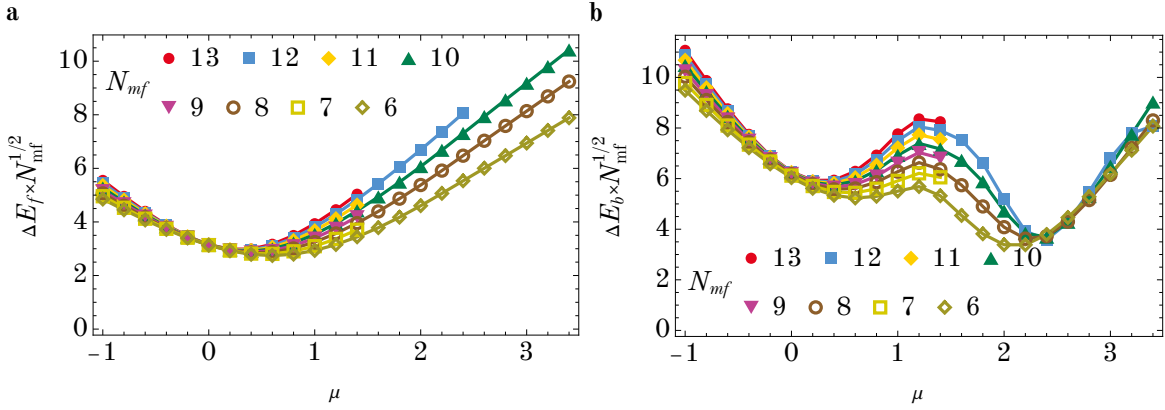


Figure 2. (a) The rescaled fermionic gap $\Delta E_f N_{mf}^{1/2}$ and (b) the rescaled bosonic gap $\Delta E_b N_{mf}^{1/2}$ as a function of μ . In the calculation, we vary N_{mf} and fix $t = 0.3$. As bPf ground state only exists for even N_{mf} , we only keep the data with $\mu < 1.5$ for odd N_{mf} .

The existence of two gapless points indicates that there is an intermediate phase whose transitions to fIQH and bPf phases are both continuous. To determine the nature of this intermediate phase, we calculate the real space entanglement spectrum with the entanglement cut at the equator [73, 74]. For a 3D gapped topological phase, the low-lying part of the ground-state entanglement spectrum for a local bipartition is generally believed [75] to reproduce the

spectral counting of the physical edge CFT of that phase. In the following, we analyse the entanglement spectrum of the three phases respectively.

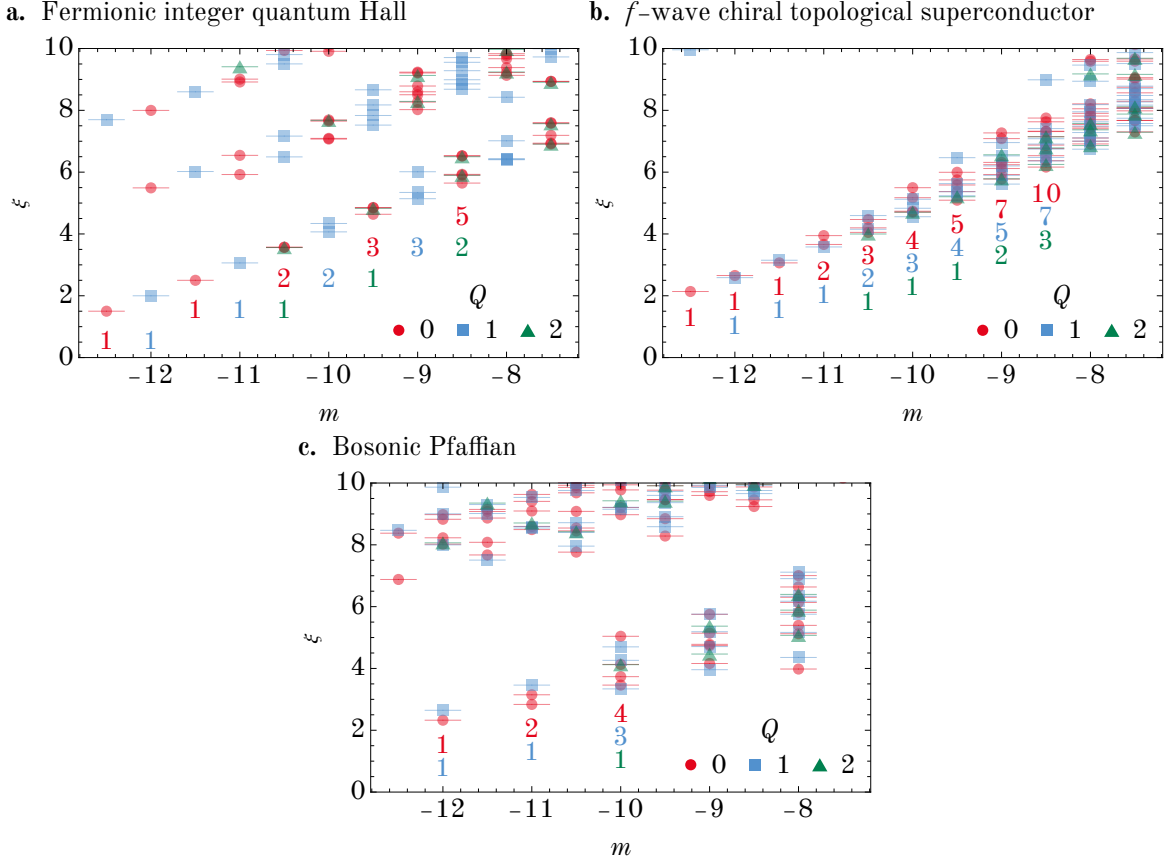


Figure 3. The real space entanglement spectrum with the cut at the equator at different phases at different charge sector $Q = (Q_{e,A} - Q_{e,B})/2$: (a) the fermionic integer quantum Hall phase at $\mu = -2$, (b) the f -wave chiral topological superconductor phase at $\mu = 1$ and (c) the bosonic Pfaffian phase at $\mu = 5$. Markers are plotted with transparency, so that nearly degenerate levels appear darker. The degeneracies for different charge sectors are labelled beneath. In the calculation we take $N_{mf} = 10$.

Fermionic integer quantum Hall phase (fIQH) The large negative μ belongs to the $\nu = 1$ fermionic integer quantum Hall phase. It can be described by a trivial Chern-Simons topological quantum field theory (TQFT) of $U(1)_1 \cong SO(2)_1$. The 2D chiral CFT on its edge is a free chiral Dirac fermion, or a pair of free chiral Majorana fermion. The two fermions form a $U(1)$ symmetry and carry charge $Q = \pm 1$. The $U(1)$ symmetry is manifest on the fuzzy sphere as

the electric charge conservation. By state-operator correspondence, the degeneracy counts in the entanglement spectrum equal the numbers of operators with corresponding $U(1)$ charge Q and angular momentum m in the chiral 2D CFT. We give the detail for the calculation from the character in Appendix A (Eq. (A.1)) and label the expected degeneracies on Figure 3. Practically Q is the half the difference $(Q_{e,A} - Q_{e,B})/2$ between the charge in two hemispheres and m is shifted by $-N_{mf}^2/8$. The counting is consistent with our numerical observation (Figure 3a).

f -wave chiral topological superconductor (TSC) We continue with the analysis of the intermediate phase. We shall show that this phase is an f -wave TSC. The f -wave TSC can be regarded as a p -wave TSC on the background of an fIQH state. In the language of Kitaev's '16-fold way' classification of topological superconductors from spinless fermion [76], the f -wave TSC has the index $\nu_K = 3$ (Chern number, or number of chiral Majorana fermions on the edge).⁸ An intuition for its origin is the fluctuating number of fermions in this phase and the pairing pattern given by H_t which antisymmetrises the orbital index of two fermions.

The TSC is described by a $SO(3)_1$ CS theory. The 2D chiral CFT on its edge is three free chiral Majorana fermions. They form a vector under a $SO(3)$ global symmetry on the edge, of which a $U(1)$ subgroup is manifest on the fuzzy sphere as the charge conservation. In the entanglement spectrum, we observe a well-split lowest chiral edge mode whose degeneracy is consistent with the 2D chiral CFT (Figure 3b, Eq. (A.2)). The TQFT has a chiral central charge $c_- = 3/2$. The enhancement from $U(1)_e$ to the $SO(3)$ global symmetry on the edge can be seen from the formation of multiplets. The excited states at $m = 1/2$ and 1 form $SO(3)$ -vectors corresponding to the Majorana fermion operator and the symmetry current.

Bosonic Pfaffian (bPf**)** The large positive μ belongs to the bosonic Pfaffian phase. The bosonic Pfaffian state is given by the many-body wavefunction on a plane with complex coordinates z, \bar{z} [54]

$$\Psi(\{z_i\}) = \text{Pf} \left(\frac{1}{z_i - z_j} \right) \prod_{i < j} (z_i - z_j) \quad (3.1)$$

⁸In this language, the p -wave TSC has $\nu_K = 1$, and the fIQH can be regarded as a d -wave TSC with $\nu_K = 2$.

where Pf is the Pfaffian of an even-dimensional square matrix, which also restricts that the bPf state is only compatible with even number of particles, *i.e.* $N_{mf} \in 2\mathbb{Z}$. It is described by a Chern-Simons theory $\text{SU}(2)_2$. As $\text{SU}(2)$ is a double covering of $\text{SO}(3)$, $\text{SO}(3)_1 \cong \text{SU}(2)_2/\mathbb{Z}_2$, *i.e.*, the $\text{SU}(2)_2$ can be regarded as gauging the \mathbb{Z}_2 fermion parity symmetry from $\text{SO}(3)_1$. Correspondingly, its chiral edge mode is the same as removing the $m \in \mathbb{Z} + \frac{1}{2}$ levels and keeping the $m \in \mathbb{Z}$ part of the chiral edge mode in $\text{SO}(3)_1$ (Figure 3c).

The $\text{SU}(2)_2$ CS theory is a non-Abelian TO with chiral central charge $c_-^{(\text{bPf})} = 3/2$ and three kinds of anyons, *viz.* \mathbb{I} , σ and ψ . They have statistical angles and fusion rules

$$\begin{aligned} \theta_{\mathbb{I}}^{(\text{bPf})} &= 0, & \theta_{\psi}^{(\text{bPf})} &= \pi, & \theta_{\sigma}^{(\text{bPf})} &= 3\pi/8 \\ \psi \times \psi &= \mathbb{I}, & \psi \times \sigma &= \sigma, & \sigma \times \sigma &= \mathbb{I} + \psi. \end{aligned} \quad (3.2)$$

Here \mathbb{I} is the vaccuum, ψ is a fermionic anyon and σ is a non-Abelian anyon. The anyons are also referred to as 0, $\frac{1}{2}$ and 1. This TO can also be understood as a Ising topological order stacked with an Abelian topological order

$$\frac{\text{Ising} \times \text{U}(1)_4}{\mathbb{Z}_2}.$$

The stacking with $\text{U}(1)_4$ adds 1 to the chiral central charge and add an additional phase $\pi/4$ to the σ anyon compared with their values $c_-^{(\text{Ising})} = 1/2$ and $\theta_{\sigma}^{(\text{Ising})} = \pi/8$ in the Ising TO. In Kitaev's '16-fold way' classification [76], this phase is described by the gauged TSC with index $\nu_K = 3$.

4 Critical Theories

In this section, we discuss the critical theories that describe the transition between the TSC and fIQH and bPf phases.

The transition from the fIQH to the TSC phase is described by a single free Majorana fermion. One way to see this is that the chiral central charge c_- increases by $1/2$ across the transition. This transition is captured by the Lagrangian

$$\mathcal{L}_{\text{Majorana}} = \frac{1}{2} \bar{\chi} (i\partial - m) \chi + \frac{5}{4} \text{CS}_g \quad (4.1)$$

where χ is a (two-component) Majorana fermion, $\bar{\chi} = \chi^T \epsilon$, $\epsilon = i\sigma^2$, and $\partial = \sigma^\mu \partial_\mu$. The gravitational Chern-Simons term is defined through extending into a 4D manifold X with the original 3D manifold its boundary $M = \partial X$ [77]

$$\int_{M=\partial X} \text{CS}_g = \frac{1}{192\pi} \int_X \text{tr} R \wedge R$$

where R is the curvature 2-form. A background CS_g level-1 comes from the background integer quantum Hall state has been included. Adding a positive/negative mass gaps out the Majorana fermion and adds an extra gravitational Chern-Simons response of level $\pm 1/4$.

$$\mathcal{L}_{\text{Majorana}}^> = \frac{3}{2} \text{CS}_g, \quad \mathcal{L}_{\text{Majorana}}^< = \text{CS}_g.$$

They recover the chiral central charge of the fIQH and TSC phases. This transition has another conjectural dual description of $\text{SO}(3)_1$ coupled to a single free scalar [78, 79]. The condensation of the scalar Higgses the gauge theory to $\text{SO}(2)_1$ describing the fIQH phase, and gapping the scalar results in $\text{SO}(3)_1$ corresponding to the TSC phase.

The transition from the TSC to the bPf phase falls into a gauged Ising (Ising*) universality, *i.e.* Ising type transition coupled to a \mathbb{Z}_2 gauge field, or the confinement transition of a \mathbb{Z}_2 gauge field. One way to understand it is to recognise that bPf can be described by TSC coupled to a \mathbb{Z}_2 gauge field, so its transition to TSC can be realised by Higgsing the \mathbb{Z}_2 gauge field. We can also use the language of CS theory to understand the emergence of gauged Ising transition. The TSC and the bPf phase can be described by $\text{SO}(3)_1 \cong \text{SU}(2)_2/\mathbb{Z}_2$ and $\text{SU}(2)_2$ respectively, and the difference is only a \mathbb{Z}_2 gauge field. So Higgsing the \mathbb{Z}_2 centre of the $\text{SU}(2)$ gauge group drives a transition from the bPf phase to the TSC phase. In Appendix B, we discuss the Lagrangian of this confinement transition. This transition can be equivalently considered in terms of anyon condensation. In the bPf phase, although the ψ anyon is fermionic, combined with the local fermion f , $f^\dagger \psi$ is bosonic with statistical angle $\theta_{f^\dagger \psi} = 0$. Across the transition, this composite particle $\langle f^\dagger \psi \rangle \neq 0$ is condensed. Due to the braiding of the anyons ψ and σ , σ will also be confined, resulting in the f -wave TSC with trivial topological order. Since this transition only changes the neutral sector, the chiral central charge $c_- = 3/2$ remains the same across the transition.

It is also worth noting that the whole phase diagram, including the three gapped phases and two critical points, can be captured by a single Lagrangian, *viz.* the adjoint QCD of $\text{SU}(2)_1$

Chern-Simons theory coupled to a fermion in the adjoint representation of the gauge group [65]. This theory has no global symmetry. When the fermion is gapped, it contributes a Chern-Simons level ± 1 depending on the sign of the mass. This drives a transition between $SU(2)_2$ topological order and a trivial topological order of $SU(2)_0$. This transition is dual to $O(1)_{-3}$ coupled to a real scalar through the level-rank duality, which is equivalent to the Ising* universality. On the other hand, the adjoint QCD has a manifest $\mathcal{N} = 1$ supersymmetry for a specific value of mass. This point falls in the phase with trivial topological order. The supersymmetry is spontaneously broken, resulting in a gapless Goldstino mode: a massless Majorana fermion. The supersymmetry is not manifest in our setup, but the Goldstino mode corresponds to the Majorana-type transition in our phase diagram.

Numerically, we verify these critical theories by inspecting the energy spectrum at the critical point. A quantum system on a sphere described by a CFT enjoys the state-operator correspondence where the scaling dimensions of the operators are proportional to the excited energies

$$\Delta_\Phi = \frac{v}{R}(E_\Phi - E_0)$$

where Φ is an arbitrary scaling operator and v is a model-dependent constant that can be determined by calibrating the stress tensor $T^{\mu\nu}$ to $\Delta = 3$. The spectrum of a CFT can be classified into multiplets of primaries and their descendants at integer spacing.

At the fIQH-TSC transition, we observe that most of the operators are close to integer level and they can be classified into multiplets of the lowest primary operators in the free Majorana fermion CFT (Figure 4a), *viz.* the fermion χ at $\Delta = 1, l = 1/2$, the relevant singlet $\bar{\chi}\chi = \epsilon_{ab}\chi^a\chi^b$ at $\Delta = 2, l = 0$, the conserved stress tensor $T^{\mu\nu} = \frac{i}{2}\bar{\chi}_a(\sigma^{(\mu})^a{}_b\partial^{\nu)}\chi^b$ at $\Delta = 3, l = 2$, $\bar{\chi}\chi\partial\chi$ at $\Delta = 4, l = 3/2$, *etc.* We highlight that spectrum contains $l \in \mathbb{Z} + \frac{1}{2}$ states corresponding to fermionic operators. The free Majorana fermion CFT will be analysed in more detail in Section 5.

At the TSC-bPf transition, although there are many non-conformal gapped excitations at relatively low energy at small system size, the low lying states for each integer $l \leq 2$ can be identified as operators in the Ising* CFT (Figure 4b). The Ising* CFT consists all the \mathbb{Z}_2 -even operators in the Ising CFT. We can identify ϵ at $\Delta = 1.412$ and its several descendants, the

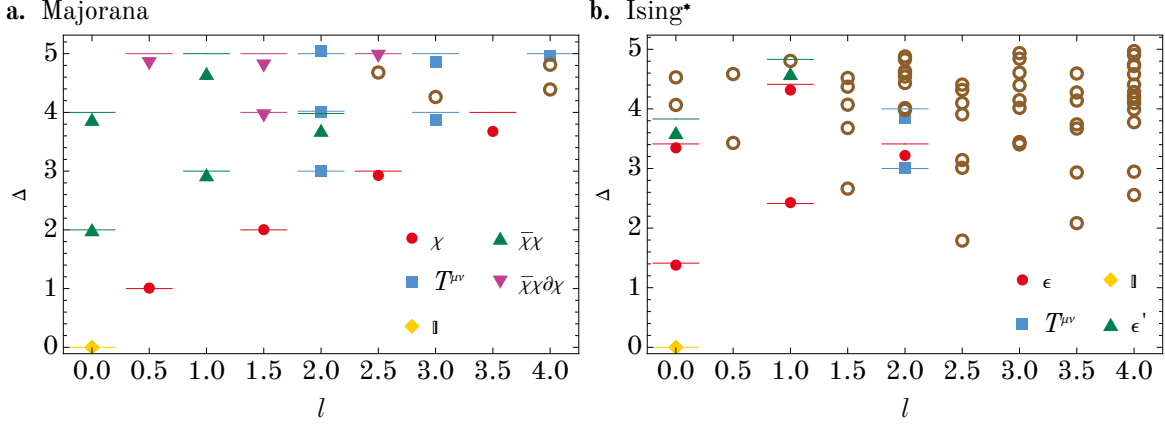


Figure 4. The rescaled energy spectrum at the conformal points (a) $t = 0.3, \mu = 0.0$ described by the free Majorana fermion CFT and (b) $t = 0.1, \mu = 2.25$ described by the Ising* CFT. We identify some multiplets of the lowest primaries in the spectra and the bars denote their expected value in the CFT. The spectra are calibrated by $\Delta_T = 3$. In the calculation, we fix $N_{mf} = 12$.

stress tensor $T^{\mu\nu}$ and ϵ' at $\Delta = 3.830$ in the spectrum. The Ising* CFT will be discussed in more detail in Section 6.

5 Free Majorana Fermion CFT

In this section, we focus on the free Majorana fermion CFT on the fuzzy sphere. In this CFT, the Majorana fermion χ has scaling dimension $\Delta = 1$ and SU(2) spin $l = 1/2$. The spectrum of scaling operator, including the primaries and descendants, can be determined with the help of harmonic oscillators [46]. Here we list the scaling dimension Δ and spin l of the low lying operators:

| | |
|--------------|----------------------------|
| $\Delta = 1$ | $l = 1/2$ |
| $\Delta = 2$ | $l = 0, 3/2$ |
| $\Delta = 3$ | $l = 1, 2, 5/2$ |
| $\Delta = 4$ | $l = 0, 3/2, 2, 2, 3, 7/2$ |
| \vdots | |

where the replicated numbers denote degenerate operators. To choose an ideal parameter point, we optimise a cost function along the critical line defined as the root mean square of the deviations of the scaling dimension of all operators with $\Delta \leq \Delta_c = 3$ from their expected values [38]. We find that in the region $0.2 < t < 0.4$, the cost function is relatively insensitive to the choice of t , and the critical $\mu_{c1} \approx 0$ up to a precision of 0.01, which may be a hint for a possible enhanced symmetry in the absence of relative chemical potential. We therefore fix $t = 0.3$ and $\mu_c = 0$.

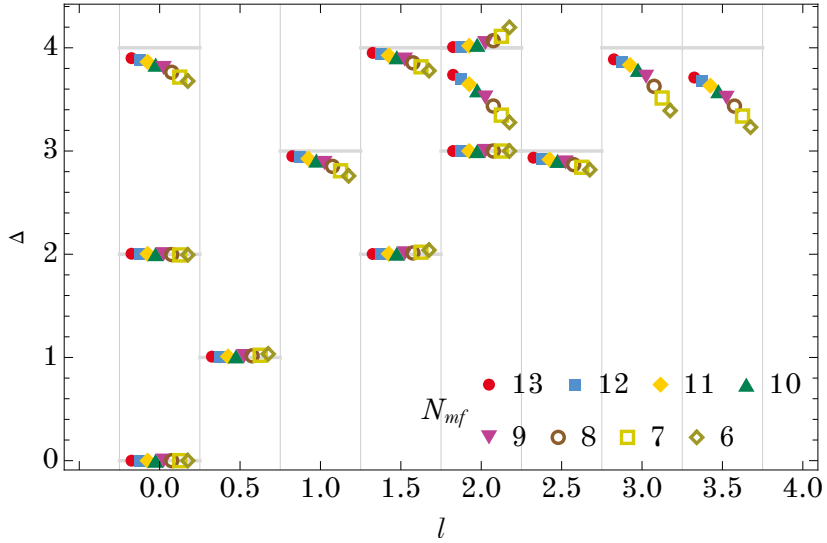


Figure 5. The spectrum with $\Delta \lesssim 4$ for various systems sizes. The scaling dimensions are calibrated by the stress tensor with $\Delta_T = 3$. The grey bars denote the theoretical value for comparison. In the calculation, we fix $t = 0.3$ and $\mu = 0$. The vertical gridlines with interval 0.5 separates different spins, which are either integers or half-integers.

We find that the low lying spectrum agrees well with the theory (Figure 5). All the states up to $\Delta = 4$ are CFT states, and all the theoretically expected operators appear in the spectrum close to integer scaling dimension. The discrepancy is within 2.5% for all the $\Delta \leq 3$ operators and most $\Delta = 4$ operators for our maximal accessible size $N_{mf} = 13$. This precision is remarkable with almost no fine-tuning at such small size even compared with similar fuzzy sphere model (*e.g.* the free real scalar [46]). With increasing system size, the scaling dimension gradually approaches to expected integer value (Figure 6a–d). We qualitatively evaluate

this through the cost function consisting of all the operators with $\Delta \leq \Delta_c = 2, 3, 4$. We find these cost functions all scale to zero as $Q \sim N_{mf}^{-\alpha/2}$ where $\alpha = 3.4, 3.6, 3.2$ respectively for $\Delta_c = 2, 3, 4$ (Figure 6e).

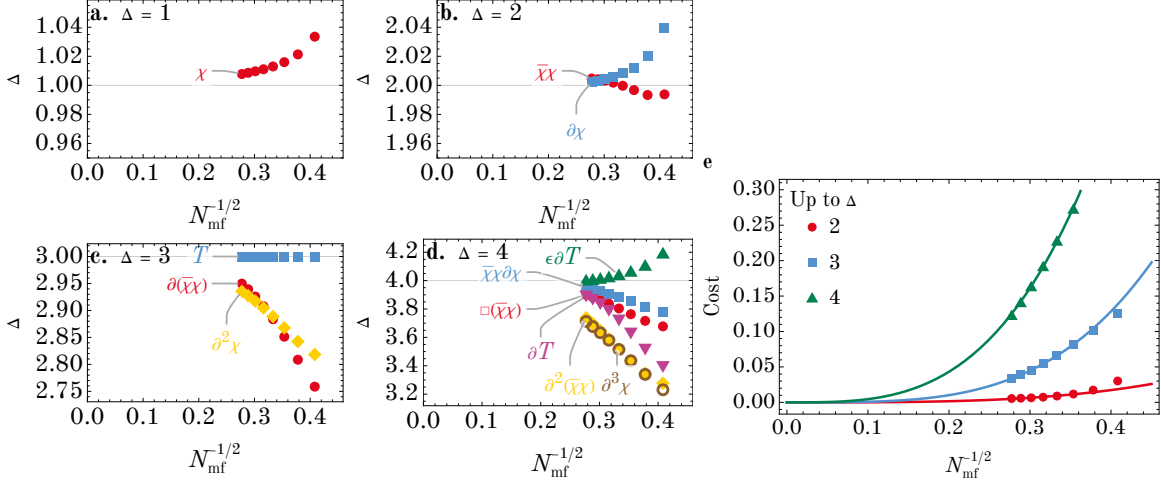


Figure 6. (a–d) The finite size scaling of scaling dimensions of various operators. The grey lines denote the theoretical value for comparison. (e) The finite size scaling of cost function consisting of operators with $\Delta \leq \Delta_c = 2, 3, 4$. In the calculation, we fix $t = 0.3$ and $\mu = 0$.

Having discussed the operator spectrum, we now move on to the correlation functions of the local operators, of which the most important is the Majorana fermion χ itself. We sketch the process here, and give the details in Appendix C. On the fuzzy sphere, the simplest gapless local fermionic operators are boson-fermion pairs $f^\dagger(\mathbf{r})b(\mathbf{r})$ and $b^\dagger(\mathbf{r})f(\mathbf{r})$. As χ is a two-component spinor, $f^\dagger b$ and $b^\dagger f$ respectively realises its two polarisations

$$\begin{aligned} f^\dagger(\mathbf{r})b(\mathbf{r}) &= \alpha\chi^{(1/2)}(\mathbf{r}) + \dots \\ b^\dagger(\mathbf{r})f(\mathbf{r}) &= \bar{\alpha}\chi^{(-1/2)}(\mathbf{r}) + \dots, \end{aligned} \quad (5.1)$$

where the two polarisations $\chi^{(s)}(\mathbf{r})$ ($s = \pm 1/2$) of the spinor carry angular momentum s under the $SO(2)$ rotation along an axis that passes \mathbf{r} (*i.e.* spin-weight), and α is a coefficient that can be determined from the microscopic model. The conformal kinematics requires the two-point correlators to have the form

$$\langle \chi^a(x_1)\bar{\chi}_b(x_2) \rangle = \frac{(\sigma_\mu)^a_b x_{12}^\mu}{(x_{12}^2)^{\Delta_\chi+1/2}}, \quad (5.2)$$

where $\Delta_\chi = 1$, $x_{1,2} \in \mathbb{R}^3$, $x_{12} = x_1 - x_2$, $a, b = \pm$ are spinor indices, and σ are the Pauli matrices. Taking the polarisations $\chi^{(s)}(\mathbf{r})$ on the sphere, their two-point function

$$\langle 0 | \chi^{\dagger(s_1)}(\mathbf{r}_1) \chi^{(s_2)}(\mathbf{r}_2) | 0 \rangle = \frac{2(-1)^{s_1} \delta_{s_1 s_2}}{R^{2\Delta_\chi} (2 \sin \frac{1}{2} \gamma_{12})^{2\Delta_\chi}} \quad (5.3)$$

has the same form as scalars on the sphere, where γ_{12} is the angular distance between the two points.

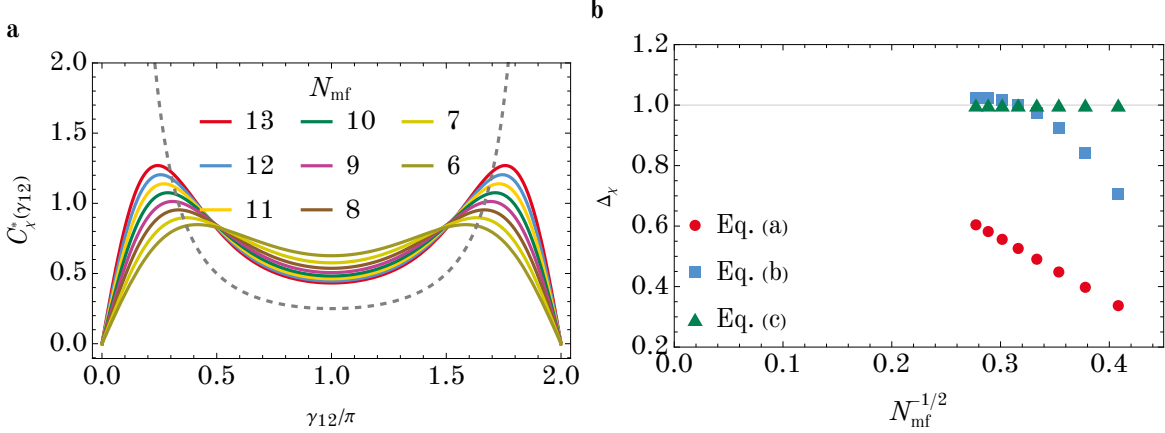


Figure 7. (a) The dimensionless correlation function Eq. (5.4) at different system sizes. The grey dashed line denotes $(2 \sin \gamma_{12}/2)^{-2}$ required by conformal symmetry. (b) The scaling dimension Δ_χ extracted from the correlation function through different ways in Eqs. (5.5) as a function of system size. In the calculation, we fix $t = 0.3$ and $\mu = 0$.

We calculate the dimensionless correlation function

$$C_\chi^*(\gamma_{12}) = \frac{1}{2i} R^{2\Delta_\chi} \langle 0 | \chi^{\dagger(1/2)}(\mathbf{r}_1) \chi^{(1/2)}(\mathbf{r}_2) | 0 \rangle. \quad (5.4)$$

whose exact expression is given in Eq. (C.25), and plot the results in Figure 7a. As the system size increases, the numerical result gradually approaches its theoretical value $(2 \sin \gamma_{12}/2)^{-2\Delta_\chi}$. From this correlation function, the scaling dimension Δ_χ can be extracted in several ways

$$C_\chi^*(\gamma_{12}) \Big|_{\gamma_{12}=\pi} = 2^{-2\Delta_\chi} \quad (5.5a)$$

$$\frac{(C_\chi^*)''(\gamma_{12})}{C_\chi^*(\gamma_{12})} \Big|_{\gamma_{12}=\pi} = \frac{\Delta_\chi}{2} \quad (5.5b)$$

$$\int_{-1}^1 d \cos \gamma_{12} \sin \frac{\gamma_{12}}{2} C_\chi^*(\gamma_{12}) = \frac{2^{2(1-\Delta_\chi)}}{3-2\Delta_\chi}. \quad (5.5c)$$

We find the results all approach $\Delta_\chi = 1$ with increasing system size (Figure 7b). The results from the integral Eq. (5.5c) has an especially small deviation within 10^{-3} at all system sizes.

We also note that under this expression of χ , the pair conversion term H_t is proportional to

$$H_t \propto \int d^2\mathbf{r} i\bar{\chi}_a(\mathbf{r})(\sigma_\mu)^a{}_b \partial^\mu \chi^b(\mathbf{r}) \quad (5.6)$$

which coincides with the kinetic term in the Hamiltonian of free Majorana fermion.

6 Gauged Ising CFT

In this section, we focus on the gauged Ising (*i. e.* Ising*) CFT on the fuzzy sphere. Gauging the \mathbb{Z}_2 symmetry brings no change to the dynamics. The operator content of the gauged Ising CFT is the \mathbb{Z}_2 -even sector in the original Ising CFT, which includes $\epsilon, T^{\mu\nu}, \text{etc.}$ The \mathbb{Z}_2 -odd operators (*e.g.* σ) of the original Ising CFT are no longer local operators in the gauged Ising CFT because they are not gauge invariant.

Numerically, we can indeed identify $\epsilon, \epsilon', T^{\mu\nu}$ and their descendants up to $\Delta < 5$ and $l \leq 2$ in the spectrum (Figure 8a). In the calculation, we fix $t = 0.1$ with a relatively optimal conformal symmetry, and choose μ for each system size by optimising a cost function consisting of $\epsilon, \partial^\mu \epsilon, \partial^\mu \partial^\nu \epsilon, \square \epsilon$ and $T^{\mu\nu}$. The optimal μ for each size is listed in Table 1 (the meaning of the right panel will be explained shortly). We note that although there are non-conformal states due to the lowest gapped excitations in the proximate bosonic Pfaffian phase, the low energy spectrum with $l \leq 2$ show relatively clear conformal signature. At large enough system size, the low energy spectrum should be dominated by CFT states and these gapped excitations will move higher, but at the sizes available, these excitations appear at relatively low energy at large l . As the bosonic Pfaffian state is only compatible with even N_{mf} , and the optimal conformal point drifts with system size, we leave the finite size scaling analysis to future work.

| N_{mf} | 12 | 10 | 8 | 13 | 11 | 9 | 7 |
|------------|-------|-------|-------|-------|-------|-------|-------|
| μ_{c2} | 2.254 | 2.230 | 2.356 | 2.290 | 2.318 | 2.373 | 2.396 |

Table 1. The optimal conformal point μ_{c2} for the Ising* CFT for each system size. In the calculation, we fix $t = 0.1$.

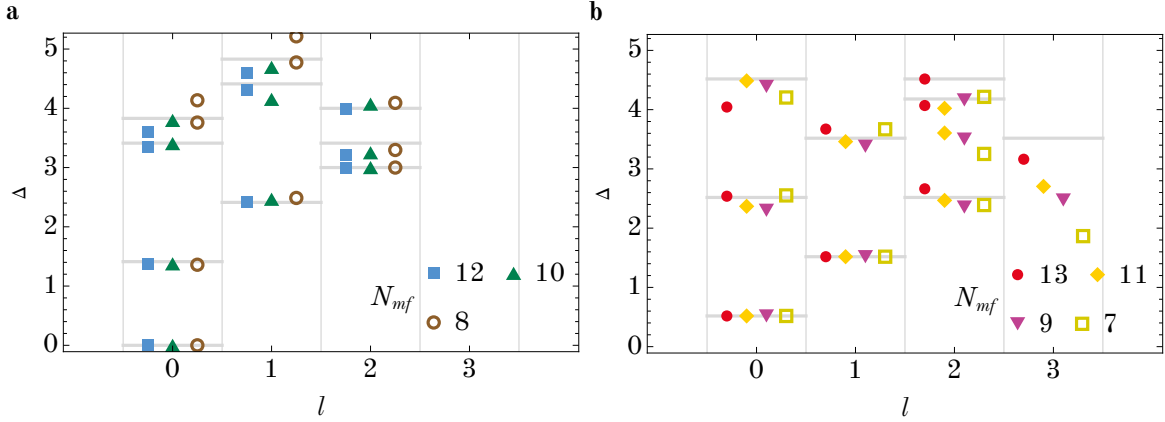


Figure 8. The spectrum of the identified CFT states with $\Delta < 5$ for various systems sizes. The grey bars denote the theoretical value for comparison. (a) The bulk spectrum at even N_{mf} corresponding to the \mathbb{Z}_2 -even part of the Ising CFT spectrum. The scaling dimensions are calibrated by the stress tensor with $\Delta_T = 3$. (b) The Wilson line endpoint spectrum at odd N_{mf} corresponding to the \mathbb{Z}_2 -odd part of the Ising CFT spectrum. The scaling dimensions are calibrated by setting $\Delta_\sigma = 0.518$ and $\Delta_{\partial^\mu \sigma} = 1.518$. In the calculation, we fix $t = 0.1$ and choose μ as in Table 1.

On the other hand, the \mathbb{Z}_2 -odd operators can be made gauge invariant by attaching a Wilson line (of \mathbb{Z}_2 gauge field) to it. In other words, the \mathbb{Z}_2 -odd operators become endpoint operators of a line defect in the gauged Ising CFT. Although the defect endpoint operators arise generically in conformal line defects and have been discussed in various contexts [30, 80–82], in the setting of \mathbb{Z}_2 (or any discrete) gauge theory, the Wilson line defect is not only conformal but also topological. In the bPf-TSC transition, we can straightforwardly realise the topological Wilson line on fuzzy sphere by leveraging the even-odd effect of N_{mf} .

We first note that the bosonic Pfaffian state is sensitive to the parity of particle number, and is only compatible with even N_{mf} . The choice of the odd N_{mf} , on the other hand, is equivalent to the insertion of a gauge charge at the centre of the sphere as the endpoint of a Wilson line defect. The reason is that although the $U(1)_e$ symmetry of electric charge conservation decouples from the dynamics at the critical point, it still has topological contribution. First, odd N_{mf} can be understood as the insertion of a 2π -flux of $U(1)_e$ on top of even N_{mf} , *i.e.*, q is increased by $1/2$. Second, the 2π -flux insertion is bound to a \mathbb{Z}_2 gauge charge. The binding of flux and gauge charge can be seen most evidently from the mutual Chern-Simons $(1/2\pi) a dA$ coupling of the

the electromagnetic field A and the dynamical gauge field a (cf. Appendix B). Here a is a $U(1)$ dynamical gauge field which is Higgsed to \mathbb{Z}_2 .⁹ Its equation of motion asserts

$$Q_a = \frac{1}{2\pi} \Phi_A$$

i.e., upon the insertion of 2π -flux of A , a \mathbb{Z}_2 gauge charge is also inserted together with an electric charge. Due to the topological nature, the attached Wilson line preserves the $SO(3)$ sphere rotation symmetry, which is different from the usual case of a non-topological conformal line. The defect endpoint operators are the \mathbb{Z}_2 -odd part of the Ising CFT, and they can be observed from the eigenstates through the state-operator correspondence on fuzzy sphere, as we will discuss below.

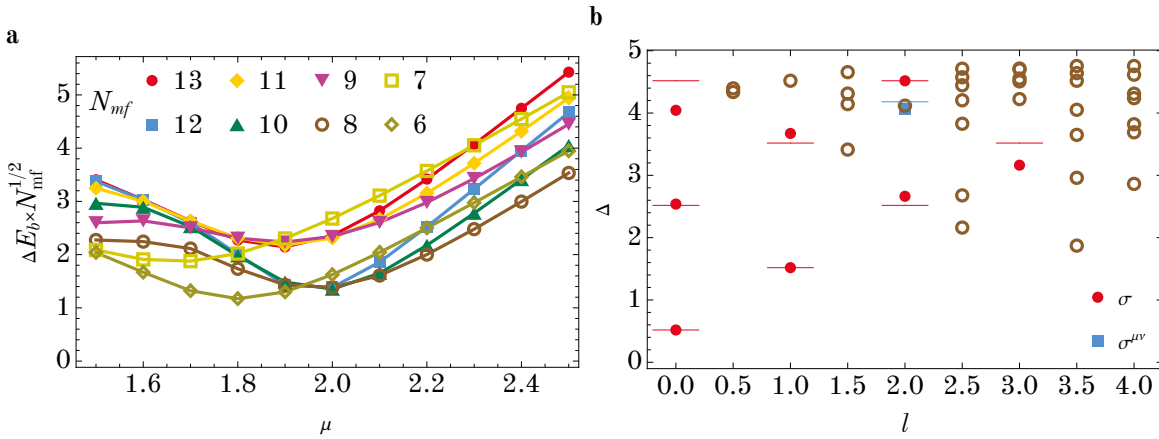


Figure 9. (a) The rescaled bosonic energy gap $\Delta E_b N_{mf}^{1/2}$ as a function of μ in vicinity of the Ising* transition for both even and odd N_{mf} calculated at $t = 0.1$. The lines with even and odd N_{mf} intersect respectively at $\mu_{c2} \approx 2.0$ except for the smallest system sizes $N_{mf} = 6, 7$. (b) The rescaled energy spectrum at conformal point $t = 0.1, \mu = 2.29$ calculated at $N_{mf} = 13$ described by the Wilson line endpoint operators in the Ising* CFT. We identify some multiplets of the lowest primaries in the spectra and the bars denote their expected value in the CFT. The energy spectrum is rescaled such that $\Delta_\sigma = 0.518$ and $\Delta_{\partial^\mu \sigma} = 1.518$.

We first confirm check the closure of the bosonic gap for the odd N_{mf} . The bosonic gap ΔE_b closes for the odd N_{mf} at $\mu_{c2} \approx 2.0$, similar to even N_{mf} , verified by overlapping $\Delta E_b \times N_{mf}^{1/2}$

⁹An equivalent way to see this Higgs mechanism is to impose $da = 0$ and $\oint_{\mathcal{C}} a = 0$ or π , where \mathcal{C} is a closed loop.

(Figure 9a). Moreover, the value of $\Delta E_b \times N_{mf}^{1/2}$ for even N_{mf} is approximately 0.7 times that for odd N_{mf} . This is consistent with the expectation from the state-operator correspondence. In the gauge-neutral sector, the lowest two spin-0 operators are vacuum \mathbb{I} and ϵ with a scaling dimension difference 1.412; in the gauge-charged sector, they are σ and $\square\sigma$ with a scaling dimension difference 2.

We then analyse the energy spectrum of the Wilson line endpoint. As the gauge charge is locked with N_{mf} , we cannot access the bulk spectrum and Wilson line endpoint spectrum at the same time and use the wavefunction overlap scheme [30, 83, 84] to extract the scaling dimension of endpoint operators. Instead, we fix the lowest endpoint operator σ at $\Delta = 0.518$, and use the second lowest operator $\partial^\mu\sigma$ at $\Delta = 1.518$ as the calibrator. The lowest operators up to $\Delta < 5$ and $l \leq 3$ can be identified with \mathbb{Z}_2 -odd operators in the Ising CFTs, *viz.* σ with $\Delta = 0.518$ and its descendants, and $\sigma^{\mu\nu}$ with $\Delta = 4.180$ (Figure 9b). Like for the gauge-neutral sector, we fix $t = 0.1$ and optimise a cost function consisting σ , $\partial^\mu\sigma$, $\partial^\mu\partial^\nu\sigma$, $\square\sigma$, $\square\partial^\mu\sigma$ and $\sigma^{\mu\nu}$ for each system size to find the optimal μ (Table 1, right panel). The spectra of identified conformal operators for each system size are plotted in Figure 8b. They agree considerably well with the odd sector of Ising CFT.

7 Discussion

In this paper, we have studied the free Majorana fermion and the gauged Ising CFT on the fuzzy sphere. We consider the setup of one bosonic and one fermionic lowest Landau level with a 1/2 angular momentum mismatch, and allow the pair conversion between them. By tuning a relative chemical potential, between a fermionic integer quantum Hall (fIQH) phase at high fermion density and a bosonic Pfaffian (bPf) phase ($SU(2)_2$ Chern-Simons theory) at high boson density, we find an intermediate phase described by an f -wave chiral topological superconductor (TSC). The three phases are separated by two continuous phase transition. Supported by numerical and theoretical evidence, we show that the fIQH-TSC transition is described by a free Majorana fermion CFT. Through state-operator correspondence, we find that the energy spectrum agrees well with the operator content of free Majorana fermion up to $\Delta \leq 4$. The local fermion operator can be realised by the combination $f^\dagger(\mathbf{r})b(\mathbf{r})$ on the sphere,

whose two-point correlation function agrees with the conformal correlator. On the other hand, the TSC-bPf transition is described by a gauged Ising (Ising*) CFT. Its spectrum agrees with the \mathbb{Z}_2 -even sector of the Ising CFT. The transition is only consistent with even N_{mf} . We find that odd N_{mf} is equivalent to the insertion of a \mathbb{Z}_2 gauge charge, and the spectrum corresponds to the Wilson line endpoint operators of the gauged Ising CFT, *i.e.* the \mathbb{Z}_2 -odd sector of the Ising CFT.

This is the first time that a CFT with critical local fermion has been realised on the fuzzy sphere. Other more interesting interacting fermionic CFTs could be studied in the future using similar setup. The simplest target would be the super-Ising CFT, which is a single Majorana fermion coupled to a real Yukawa field σ . The \mathbb{Z}_2 symmetry of σ is locked with parity due to the Yukawa coupling $\sigma\bar{\chi}\chi$. This theory has enhanced $\mathcal{N} = 1$ supersymmetry, where σ , χ and $\epsilon = \sigma^2$ combines into a superconformal multiplet. Our current setup does not have a manifest parity symmetry, so one has to tune at least three relevant operators, *viz.* σ , ϵ , and σ' . Finding a way to implement the parity for Majorana fermion would greatly help targeting this CFT. Another noticeable direction is to generalise this phase diagram as $SU(2)_1$ coupled to an adjoint fermion to other adjoint QCDs [65], which may describe more exotic phase transitions.

In addition, Chern-Simons-matter theories with fermionic content is also an interesting target for fuzzy sphere. For example, the confinement transition of $\nu = 1/3$ Laughlin state which describes its transition with a trivially gapped, has 2π -monopole with spin-3/2 [85] which may be enhanced to the supercurrent in a $\mathcal{N} = 2$ supersymmetry, but the dual supersymmetric theory is expected to be gapped [86]. Another series of examples are the QED with Chern-Simons coupling [20], which describe transitions between Jain states [87]. For example, the $N_f = 3$ QED describes the transition between the states with fillings $\nu = 1/3$ and $\nu = 2/3$, and has 4π -monopoles with spin-1/2 and 3/2. Fuzzy sphere is a promising platform to study these theories, as the realisation of the proximate topological orders are natural with the fractional quantum Hall setup, *e.g.*, the Laughlin states [88] with filling $\nu = 1/k$ realise the Abelian topological orders captured by Chern-Simons theories $U(1)_{-k}$, the Jain sequence [87] with $\nu = p/(mp + 1)$ realises the Abelian topological orders with composite fermion descriptions, and the Read-Rezayi sequence with $\nu = p/(mp + 2)$ [89], as a natural extension of the Moore-Read states [54], realises in general a series of non-Abelian topological orders.

Our work also represents a step towards studying renormalisable Lagrangians of quantum field theories on the fuzzy sphere. Most of the fuzzy sphere works so far are limited to realising universalities by constructing Hamiltonian with correct symmetry and anomaly and letting it flow to the desired conformal fixed point in the IR. In the meantime, realising renormalisable Lagrangians within the fuzzy sphere framework will be the cornerstone towards QFT questions like field theory duality. A natural starting point is to understand free theories on fuzzy sphere, such as the free fermion CFT studied here as well as free real scalar CFT in Ref. [46]. Our fuzzy sphere Majorana fermion model has several interesting features which deserve further exploration:

1. The critical point lies at $\mu_{c1} = 0$ at high precision for a wide range of t , hinting at some enhanced symmetry that forbids the chemical potential for the free Majorana fermion CFT.
2. The Hamiltonian at the critical point $\mu_{c1} = 0$ resembles the familiar free Majorana fermion QFT. Specifically, apart from the charge density interaction term n_e^2 , the Hamiltonian takes the form $\bar{\chi}i\partial\chi$, where χ denotes the Majorana fermion.
3. Just like the density operators, the angular components of the local fermion $\eta_{lm}^{(1/2)} = \int d^2\mathbf{r} \bar{Y}_{lm}^{(1/2)}(\mathbf{r})f^\dagger(\mathbf{r})b(\mathbf{r})$ could have an algebraic structure similar to that of the density operator in fermion bilinear. In particular, it would be interesting to determine whether this algebra is a deformation of the fermionic harmonic oscillator, analogous to the free scalar on the fuzzy sphere [46]. Following this line, the ground state could be described by a wavefunction ansatz resembling a coherent state of η , as in the case of the free scalar.

Understanding these features may guide us to generalise the fuzzy sphere approach to other interacting Lagrangians. The simplest type of interaction to target could be the Yukawa coupling. Another route is to engineer the spin-1 gauge field and then construct the critical gauge theories.

Moving on to the Ising* transition, we explicitly demonstrate the physics of a topological defect of a CFT on the fuzzy sphere. Moreover, the gauging of the \mathbb{Z}_2 symmetry offers opportunities to study conformal line defects in the Ising CFT. For example, the monodromy defect in 3d Ising CFT [90] is attached to a half-infinite topological plane across which a \mathbb{Z}_2 twist is inserted. After gauging the \mathbb{Z}_2 symmetry, it becomes the vortex line of the \mathbb{Z}_2 gauge field which is no longer attached to the topological plane. This means that it can be realised locally

at antipodal points on the fuzzy sphere. The vortex line at the Ising* transition is closely related to the σ anyon in the proximate bPf phase: once the bulk is gapped, the vortex line becomes the σ worldline; under radial quantisation, this appears as two σ anyons localised at the poles. The attempt to trap and separate anyons [91] in the $\nu = 5/2$ FQH state may hint us how to realise the vortex line in the Ising* CFT trap anyons in the bPf phase. Another interesting related question to explore is the self-dual confinement transition in the \mathbb{Z}_2 topological order [92]: While condensing e or m alone in the \mathbb{Z}_2 TO drives an Ising* type transition to the trivially gapped phase, the transition condensing the e and m anyon at the same time in a self-dual manner may fall in a different universality. Its nature attracts wide attention, and a few critical exponents have been computed in lattice models through Monte Carlo [93]. This question could be potentially addressed on the fuzzy sphere, as the \mathbb{Z}_2 topological order could be produced by coupling the $SU(2)_2$ (*i.e.* bPf) to its opposite-chirality partner $SU(2)_{-2}$ and condensing certain types of anyons.

Critical theories with a discrete symmetry gauged also exist in other quantum Hall systems. One example is the direct continuous transition between $\nu_f = 1$ fIQH state and $\nu_b = 1/4$ bosonic Laughlin state, which was previously studied theoretically [94] and numerically [95]. These two phases can respectively be identified as the $\nu_K = 2$ TSC and the \mathbb{Z}_2 -gauged $\nu_K = 2$ TSC in the Kitaev's 16-fold way language. The $1/4$ bosonic Laughlin state, described by a $U(1)_{-4}$ Chern-Simons theory, has four types of anyons with statistical angles $\theta_k = \pi k^2/4$ ($k = 0, 1, 2, 3$). The condensation of the fermionic $k = 2$ anyon combining with the local fermion confines the other anyons and drive the transition towards fIQH, a scenario analogous to the TSC-bPf transition in our setup. More generally, we conjecture that the $\nu_f = 1$ fIQH to $\nu = 1/k^2$ Laughlin state could be described by a gauged Potts universality at $k = 3$ or a $O(2)$ Wilson-Fisher coupled to a \mathbb{Z}_k gauge field at higher k .

Acknowledgments

We would like to thank Jaume Gomis, Zixiang Hu, Ryan Lanzetta, Zlakto Papić, Subir Sachdev, Chong Wang, Zechuan Zheng, Wei Zhu, and Yijian Zou for fruitful discussions. Z.Z. acknowledges support from the Natural Sciences and Engineering Research Council of

Canada (NSERC) through Discovery Grants. Research at Perimeter Institute is supported in part by the Government of Canada through the Department of Innovation, Science and Industry Canada and by the Province of Ontario through the Ministry of Colleges and Universities. The numerical calculations are done using the package Fuzzified [72].

Note added Upon preparing this manuscript, we become aware of a parallel study [96] that investigates the gauged Majorana CFT (which is bosonic) in a different setup of quantum Hall bilayer transition.

A Edge CFT Character and Entanglement Spectrum Degeneracy Count

In this section, we give the detail on calculating the degeneracy count for the entanglement spectrum in Section 3 and Figure 3 from the character of the 2D chiral CFTs on the edge.

Fermionic integer quantum Hall phase (fIQH) is described by $U(1)_1 \cong SO(2)_1$. The 2D chiral CFT on its edge is a pair of free chiral Majorana fermion that form a $U(1)$ symmetry and carry charge $Q = \pm 1$. The character of the edge CFT is

$$\begin{aligned}
\chi^{(\text{fIQH})}(q, y) &= \prod_{Q=\pm 1} q^{1/48} \prod_{k \in \mathbb{Z} + 1/2} (1 + y^Q q^k) \\
&= q^{1/24} (1 + yq^{1/2} + y^{-1}q^{1/2} + y^2q^2 + y^{-2}q^2 + \dots) \\
&\quad \times (1 + q + 2q^2 + 3q^3 + 5q^4 + 7q^5 + 11q^6 + \dots) \\
&= q^{1/24} (1 + q + 2q^2 + 3q^3 + 5q^4 + 7q^5 + 11q^6 + \dots \\
&\quad + yq^{1/2} + yq^{3/2} + 2yq^{5/2} + 3yq^{7/2} + 5yq^{9/2} + \dots \\
&\quad + y^{-1}q^{1/2} + y^{-1}q^{3/2} + 2y^{-1}q^{5/2} + 3y^{-1}q^{7/2} + 5y^{-1}q^{9/2} + \dots \\
&\quad + y^2q^2 + y^2q^3 + 2y^2q^4 + 3y^2q^5 + 5y^2q^6 + \dots \\
&\quad + y^{-2}q^2 + y^{-2}q^3 + 2y^{-2}q^4 + 3y^{-2}q^5 + 5y^{-2}q^6 + \dots \\
&\quad + \dots)
\end{aligned} \tag{A.1}$$

Here $y = e^{2\pi iz}$ and z is the fugacity that couples to the $U(1)$. Its chiral central charge is $c_- = 1$. By state-operator correspondence, the coefficient in front of $y^Q q^{m-c_-/24}$ is the degeneracy in the entanglement spectrum with angular momentum m in z -direction (compared with the ground

state) and electric charge Q . The factorisation shows that the chiral edge modes in different charge sector have the same degeneracy but have the momentum m shifted.

f -wave chiral topological superconductor (TSC) is described by $\text{SO}(3)_1$. The 2D chiral CFT on its edge is three free chiral Majorana fermions. They form a vector under a $\text{SO}(3)$ global symmetry on the edge, of which a $\text{U}(1)$ subgroup is manifest on the fuzzy sphere. Its character is

$$\begin{aligned}
\chi^{(\text{TSC})}(q, y) &= \prod_{Q=0,\pm 1} q^{1/48} \prod_{k \in \mathbb{Z} + 1/2} (1 + y^Q q^k) \\
&= q^{1/16} (1 + yq^{1/2} + y^{-1}q^{1/2} + y^2q^2 + y^{-2}q^2 + \dots) \\
&\quad \times (1 + q^{1/2} + q + 2q^{3/2} + 3q^2 + 4q^{5/2} + 5q^3 + 7q^{7/2} \dots) \\
&= q^{1/16} (1 + q^{1/2} + q + 2q^{3/2} + 3q^2 + 4q^{5/2} + 5q^3 + 7q^{7/2} + \dots \\
&\quad + yq^{1/2} + yq + yq^{3/2} + 2yq^2 + 3yq^{5/2} + 4yq^3 + 5yq^{7/2} + \dots \\
&\quad + y^{-1}q^{1/2} + y^{-1}q + y^{-1}q^{3/2} + 2y^{-1}q^2 + 3y^{-1}q^{5/2} + 4y^{-1}q^3 + \dots \\
&\quad + y^2q^2 + y^2q^{5/2} + y^2q^3 + 2q^{7/2} + 3y^2q^4 + 4y^2q^{9/2} + 5y^2q^5 + \dots \\
&\quad + y^{-2}q^2 + y^{-2}q^{5/2} + y^{-2}q^3 + 2q^{7/2} + 3y^{-2}q^4 + 4y^{-2}q^{9/2} + \dots \\
&\quad + \dots) \tag{A.2}
\end{aligned}$$

Bosonic Pfaffian (bPf) is described by $\text{SU}(2)_2$. As $\text{SU}(2)$ is a double covering of $\text{SO}(3)$, $\text{SO}(3)_1 \cong \text{SU}(2)_2/\mathbb{Z}_2$, *i.e.*, the $\text{SU}(2)_2$ can be regarded as gauging the \mathbb{Z}_2 fermion parity symmetry from $\text{SO}(3)_1$. Correspondingly, on its edge

$$\begin{aligned}
\chi^{(\text{bPf})}(q, y) &= \frac{1}{2} \left[\chi^{(\text{TSC})}(q, y) \pm (q^{1/2} \rightarrow -q^{1/2}) \right] \\
&= (\chi^{(\text{TSC})}(q, y) \text{ with only } \mathbb{Z} \text{ (or } \mathbb{Z} + \frac{1}{2} \text{) power of } q) \\
&= q^{1/16} (q^{1/2} + 2q^{3/2} + 4q^{5/2} + 7q^{7/2} + \dots \\
&\quad + yq^{1/2} + yq^{3/2} + 3yq^{5/2} + 5yq^{7/2} + \dots \\
&\quad + y^{-1}q^{1/2} + y^{-1}q^{3/2} + 3y^{-1}q^{5/2} + 5y^{-1}q^{7/2} \dots \\
&\quad + y^2q^{5/2} + 2q^{7/2} + 4y^2q^{9/2} + \dots \\
&\quad + y^{-2}q^{5/2} + 2q^{7/2} + 4y^{-2}q^{9/2} + \dots
\end{aligned}$$

$$+ \dots) \quad (\text{taking } - \text{ and } \mathbb{Z} + \frac{1}{2} \text{ for } N_{mf} \in 4\mathbb{Z} + 2). \quad (\text{A.3})$$

The choice of \pm depends on whether the ground state of the chiral CFT on the edge is shifted to an integer or half-integer m , *i.e.* $+$ for $N_{mf} \in 4\mathbb{Z}$ and $-$ for $N_{mf} \in 4\mathbb{Z} + 2$. Its chiral edge mode is the same as removing the $m \in \mathbb{Z} + \frac{1}{2}$ levels and keeping the $m \in \mathbb{Z}$ part of the chiral edge mode in $\text{SO}(3)_1$.

B Lagrangian Description of the Gauged Ising Transition

In this section, we construct a Lagrangian that captures the transition between the bPf phase described by $\text{SU}(2)_2$ and the TSC phase described by $\text{SU}(2)_2/\mathbb{Z}_2 \cong \text{SO}(3)_1$. We consider a $\text{U}(2)$ gauge field $\alpha + \frac{1}{2}a\mathbb{I}_2$ where α is the traceless part and a is the trace part.

$$S = \int \frac{2}{4\pi} \text{tr} (\alpha d\alpha + \frac{2}{3}\alpha^3) + \frac{1}{4\pi}a da + \frac{2}{2\pi}b da + \frac{1}{2\pi}A da + \frac{1}{4\pi}A dA + d^3x \left[((\partial_\mu - ia_\mu)\phi)^2 + \frac{m^2}{2}\phi^2 + \frac{\lambda}{4!}\phi^4 \right] \quad (\text{B.1})$$

We start with the

$$\text{U}(2)_{2,1} = \frac{\text{SU}(2)_2 \times \text{U}(1)_2}{\mathbb{Z}_2}$$

Chern-Simons theory. The trace part a is coupled to the electromagnetic field A . We couple a to another dynamical $\text{U}(1)$ gauge field b through a mutual Chern-Simons coupling. This coupling will Higgs a from $\text{U}(1)$ to \mathbb{Z}_2 . This can be seen from

1. The equation of motion of b asserts that $da = 0$, and
2. The insertion of a Wilson line of b enforces an a -flux $\oint a \in \pi\mathbb{Z}$ around it.

This \mathbb{Z}_2 gauge field is now the centre of the $\text{SU}(2)$. We then couple the \mathbb{Z}_2 gauge field a to a real scalar ϕ . The phase transition is controlled by the mass of the scalar.

1. When $m^2 > m_c^2$, the scalar field is gapped, and the \mathbb{Z}_2 gauge field remains. The resulting theory is $(\text{SU}(2)_2 \times \mathbb{Z}_2)/\mathbb{Z}_2 = \text{SU}(2)_2$, which describes the topological order of bosonic Pfaffian phase.
2. When $m^2 < m_c^2$, the scalar field is condensed, this confines the \mathbb{Z}_2 gauge field. The resulting theory is $\text{SU}(2)_2/\mathbb{Z}_2 = \text{SO}(3)_1$, which describes the f -wave TSC.

C Realisation of Local Spinor Operators on the Fuzzy Sphere

The local Majorana fermion χ is a two-component spinor,

$$\chi(\mathbf{r}) = (\{\chi^M(\mathbf{r})\}_{M=\pm 1/2})^T = \begin{pmatrix} \chi^{-1/2}(\mathbf{r}) \\ \chi^{1/2}(\mathbf{r}) \end{pmatrix}. \quad (\text{C.1})$$

Here we denote the two components by an angular momentum index $M = \pm 1/2$, such that acting each component at the origin point will get us an eigenstate

$$\begin{pmatrix} \chi^{-1/2}(0) \\ 0 \end{pmatrix} |\mathbb{I}\rangle = |\chi_{l=1/2, m=-1/2}\rangle, \quad \begin{pmatrix} 0 \\ \chi^{1/2}(0) \end{pmatrix} |\mathbb{I}\rangle = |\chi_{l=1/2, m=1/2}\rangle.$$

At each point on the sphere,

$$\chi(\mathbf{r}) = \chi^{(+1/2)}(\mathbf{r})\mathbf{e}_{(1/2)} + \chi^{(-1/2)}(\mathbf{r})\mathbf{e}_{(-1/2)}, \quad (\text{C.2})$$

where the two polarisations $\chi^{(s)}(\mathbf{r})$ ($s = \pm 1/2$) of the spinor carry angular momentum s under the rotation along an axis that passes \mathbf{r} . Their polarisation vectors can be written as

$$e_{(s)}^M = D_{sM}^{1/2}(0, \theta, \phi) = (-1)^{-s} Y^{(-s), 1/2, M}(\mathbf{r}) \quad (\text{C.3})$$

Specifically,

$$\mathbf{e}_{(-1/2)} = \begin{pmatrix} u \\ -v \end{pmatrix}, \quad \mathbf{e}_{(+1/2)} = \begin{pmatrix} \bar{v} \\ \bar{u} \end{pmatrix}. \quad (\text{C.4})$$

Here $u = e^{-i\phi/2} \cos \theta/2$ and $v = e^{i\phi/2} \sin \theta/2$ compose the Hopf spinor. $(\mathbf{e}_{(-1/2)}(\mathbf{r}), \mathbf{e}_{(1/2)}(\mathbf{r}))$ is an orthonormal basis for spinor fields on the sphere. They satisfy

$$\bar{\mathbf{e}}^{(s)} \mathbf{e}_{(s')} = \delta_{s'}^s, \quad \bar{\mathbf{e}}^{(s)} = (-1)^{-s} \mathbf{e}_{(-s)}^T \mathbf{g}, \quad g_{mm'} = \delta_{m+m', 0} (-1)^{-m}. \quad (\text{C.5})$$

Altogether, $(\mathbf{e}_{(-1/2)}, \mathbf{e}_{(1/2)})$ composes the Wigner's D -matrix $D^l(\theta, \phi, \psi)$ with $l = 1/2$ and $\psi = 0$, which is a unitary matrix used to rotate spinning objects around the globe.

Here we explain some of the notations. The indices in the parentheses are the spin weight. The expression altogether must carry spin-weight 0. We use a rule that the lower indices lower the angular momentum or spin weight and the upper indices raise them. The indices of spherical

harmonics shall also be adapted to this rule. The indices are raised and lowered with a rule such that

$$u^m = (-1)^m u_{-m}, \quad u_m = (-1)^{-m} u^{-m}. \quad (\text{C.6})$$

The indices of the spherical harmonics follow the same logic, which makes it a bit different from the standard notation. This notation helps us keep track of all the conjugation relations and minus signs, *e.g.*, the conjugation of spherical harmonics is automatically taken care of

$$\bar{Y}_{(s),l,m} = (-1)^{-s-m} Y^{(-s),l,-m}$$

as well as the orthonormal relations

$$e_m^{(s')} e_{(s)}^m = \delta_s^{s'}.$$

The polarisation can be decomposed into spherical components on the basis of spin-weighted spherical harmonics.

$$\begin{aligned} \chi^{(s)}(\mathbf{r}) &= \frac{1}{R^2} \sum_{l=1/2}^{\infty} \sum_{m=-l}^l \chi^{(s),l,m} Y^{(s),l,m}(\mathbf{r}) \\ \chi^{(s),l,m} &= \int d^2\mathbf{r} \bar{Y}_{(s),l,m}(\mathbf{r}) \chi^{(s)}(\mathbf{r}). \end{aligned} \quad (\text{C.7})$$

Now we consider the two-point correlation functions of χ . In the standard notation, the conformal kinematics requires

$$\langle \chi^a(x_1) \chi^b(x_2) \rangle = \frac{\sigma_\mu^{ab} x_{12}^\mu}{(x_{12}^2)^{3/2}}, \quad (\text{C.8})$$

where $x_{1,2} \in \mathbb{R}^3$, $x_{12} = x_1 - x_2$, a, b are spinor indices, and σ are the Pauli matrices. It can be equivalently written as

$$\langle \chi^{m_1}(x_1) \chi^{m_2}(x_2) \rangle = \frac{\sqrt{2} C_{1,m}^{\frac{1}{2}m_1; \frac{1}{2}m_2} \hat{x}_{12}^m}{(x_{12}^2)^2} \quad (\text{C.9})$$

where

$$\begin{aligned} \hat{x}^m &= \sqrt{\frac{4\pi}{3}} Y^{1m}(\hat{x}) = \left(\frac{1}{\sqrt{2}} e^{-i\phi} \sin \theta, \cos \theta, -\frac{1}{\sqrt{2}} e^{i\phi} \sin \theta \right)^T \\ &= C_{10}^{\frac{1}{2}s_1; \frac{1}{2}s_2} C_{\frac{1}{2}m_1; \frac{1}{2}m_2}^{1m} e_{(s_1)}^{m_1}(\hat{x}) e_{(s_2)}^{m_2}(\hat{x}), \end{aligned} \quad (\text{C.10})$$

and $C_{lm}^{l_1 m_1; l_2 m_2}$ is the Clebsh-Gordan coefficient. We use this notation such that the contraction of indices are clearer.

We first consider the case where x_2 is at the origin point and x_1 is on the unit sphere. After Weyl transformation, it can be measured through the matrix element $\langle 0 | \chi^{(s)}(\mathbf{r}) | \chi^m \rangle$ on the fuzzy sphere.

$$\langle 0 | \chi^{(s)}(\mathbf{r}) | \chi^m \rangle = \frac{1}{R} e_{m'}^{(s)} \langle \chi^m(\mathbf{r}) \chi^{m'}(0) \rangle = \frac{R^{-1}}{\sqrt{2\pi}} Y^{(s) \frac{1}{2} m}(\mathbf{r}). \quad (\text{C.11})$$

Hence, for the spherical components,

$$\langle 0 | \chi^{(s) l' m'} | \chi^m \rangle = \frac{R^{-1}}{\sqrt{2\pi}} \delta_{l', \frac{1}{2}} (-1)^m \delta_{m' + m, 0}. \quad (\text{C.12})$$

We then consider the case where both points are on the unit sphere. After the Weyl transformation, it can be measured through $\langle 0 | \chi^{(s_1)}(\mathbf{r}_1) \chi^{(s_2)}(\mathbf{r}_2) | 0 \rangle$ on the fuzzy sphere.

$$\begin{aligned} \langle 0 | \chi^{(s_1)}(\mathbf{r}_1) \chi^{(s_2)}(\mathbf{r}_2) | 0 \rangle &= R^{-2} e_{m_1}^{(s_1)}(\mathbf{r}_1) e_{m_2}^{(s_2)}(\mathbf{r}_2) \langle \chi^{m_1}(x_1) \chi^{m_2}(x_2) \rangle \\ &= 2i \delta_{s_1 + s_2, 0} x_{12}^{-2} \\ \langle 0 | \chi_{(s_1)}(\mathbf{r}_1) \chi^{(s_2)}(\mathbf{r}_2) | 0 \rangle &= 2(-1)^{1/2 - s_1} \delta_{s_2}^{s_1} x_{12}^{-2}. \end{aligned} \quad (\text{C.13})$$

Hence, the correlation function of each spin-weighted component behaves exactly like a scalar correlator. In terms of the spherical components,

$$\begin{aligned} \langle 0 | \chi_{(s)} \chi^{(s)}(\mathbf{r}_2) | 0 \rangle &= \sum_{l_1 m_1 l_2 m_2} \langle \chi_{(s)} l_1 m_1 \chi^{(s) l_2 m_2} \rangle \bar{Y}_{(s) l_1 m_1}(\mathbf{r}_1) Y^{(s) l_2 m_2} \\ &= \sum_{l_1 m_1 l_2 m_2} \langle \chi_{(s)} l_1 0 \chi^{(s) l_1 0} \rangle \delta_{l_1 m_1}^{l_2 m_2} \bar{Y}_{(s) l_1 m_1}(\mathbf{r}_1) Y^{(s) l_2 m_2} \\ &= \sum_l \langle \chi_{(s)} l 0 \chi^{(s) l 0} \rangle \sum_m \bar{Y}_{(s) l m}(\mathbf{r}_1) Y^{(s) l m}(\mathbf{r}_2) \end{aligned} \quad (\text{C.14})$$

where the second line comes from the rotation symmetry. To perform the summation, we express the spherical Harmonics in terms of the D -matrix

$$\begin{aligned} Y^{(s) l m}(\mathbf{r}_2) &= (-1)^s D_{-s, m}^l(0, \theta_2, \phi_2) \\ \bar{Y}_{(s) l m}(\mathbf{r}_1) &= (-1)^{-l} \bar{Y}_{(-s) l, m}(-\mathbf{r}_1) \\ &= (-1)^{-l-s} \bar{D}_{s m}^l(0, \pi - \theta_1, \pi + \phi_1) \end{aligned}$$

$$\begin{aligned}
& = (-1)^{-l-s} D_{ms}^l(-\pi - \phi_1, -\pi + \theta_1, 0) \\
\sum_m \bar{Y}_{(s)lm}(\mathbf{r}_1) Y^{(s)lm}(\mathbf{r}_2) & = (-1)^{-l} (D^l(0, \theta_2, \phi_2) D^l(-\pi - \phi_1, -\pi + \theta_1, 0))_{-s,s} \\
& = (-1)^l D_{-s,s}^l(\psi', \pi - \gamma_{12}, \phi') \\
& = (-1)^l e^{is(\phi' - \psi')} d_{-s,s}^l(\pi - \gamma_{12}) \\
& = e^{is(\phi' - \psi')} d_{-s,s}^l(\gamma_{12}) \\
& = e^{is(\phi' - \psi')} \frac{2l+1}{4\pi} \left(\sin \frac{\gamma_{12}}{2} \right)^{2s} P_{l-s}^{(2s,0)}(\cos \gamma_{12}). \tag{C.15}
\end{aligned}$$

In the last line, we only calculate for positive s , and negative s follows similarly. There is an overall phase that depends on the relative position of the two points, so we focus on the amplitude. In the third last line, we have used the superposition of rotations, and γ_{12} is the angular distance between the two points. The $P_n^{(\alpha,0)}$ are the Jacobi polynomials. They are defined on the interval $[-1, 1]$ and has orthonormal relation

$$\int d\Omega \sin^{2s} \frac{\theta}{2} P_{l-s}^{(2s,0)}(\cos \theta) P_{l'-s}^{(2s,0)}(\cos \theta) = \frac{4\pi}{2l+1} \delta_{ll'}. \tag{C.16}$$

The components are

$$C_\chi(\gamma_{12}) = \langle 0 | \chi_{(1/2)}(\mathbf{r}_1) \chi^{(1/2)}(\mathbf{r}_2) | 0 \rangle = \sum_l C_{\chi,l} \frac{2l+1}{4\pi} \sin \frac{\gamma_{12}}{2} P_{l-1/2}^{(1,0)}(\cos \gamma_{12}) \tag{C.17}$$

$$C_{\chi,l} = 2\pi \int \sin \gamma_{12} d\gamma_{12} C_\chi(\gamma_{12}) \sin \frac{\gamma_{12}}{2} P_{l-1/2}^{(1,0)}(\cos \gamma_{12}). \tag{C.18}$$

For $C_\chi(\gamma_{12}) = (2 \sin \gamma_{12}/2)^{-2}$, the decomposed components are

$$C_{\chi,l} = 2\pi.$$

We then briefly discuss how to decompose the local fermionic operators on the fuzzy sphere

$$\eta^{(1/2)}(\mathbf{r}) = f^\dagger(\mathbf{r}) b(\mathbf{r}), \quad \eta^{(-1/2)}(\mathbf{r}) = f^\dagger(\mathbf{r}) b(\mathbf{r}) \tag{C.19}$$

into spherical components:

$$\begin{aligned}
\eta^{(1/2)}(\mathbf{r}) & = \eta^{(1/2)lm} Y^{(1/2)lm}(\mathbf{r}) \\
\eta^{(1/2)lm} & = \int d^2 \mathbf{r} \bar{Y}_{(1/2)lm} \eta^{(1/2)}(\mathbf{r}) \tag{C.20}
\end{aligned}$$

$$\begin{aligned}
&= \int d^2 \mathbf{r} \bar{Y}_{(1/2)lm} f^\dagger(\mathbf{r}) b(\mathbf{r}) \\
&= \sum_{m_1 m_2} f^{\dagger m_1} b_{m_2} \int d^2 \mathbf{r} \bar{Y}_{(1/2)lm} Y^{(q)qm_1} \bar{Y}_{(q-1/2),q-1/2,m_2} \\
&= \sum_{m_1 m_2} f^{\dagger m_1} b_{m_2} \delta_{m_1, m_2 + m} (-1)^{-q-m_1} \\
&\quad \times \sqrt{\frac{2q(2q+1)(2l+1)}{4\pi}} \begin{pmatrix} l & q & q - \frac{1}{2} \\ m & -m_1 & m_2 \end{pmatrix} \begin{pmatrix} l & q & q - \frac{1}{2} \\ 1/2 & -q & q - \frac{1}{2} \end{pmatrix}. \quad (\text{C.21})
\end{aligned}$$

The $\eta^{(-1/2)}$ follows similarly.

The $\eta^{(\pm 1/2)}$ realises the two polarisations of χ

$$\eta^{(1/2)} = \alpha \chi^{(1/2)}(\mathbf{r}) + \dots \quad (\text{C.22})$$

The coefficient α can be settled through Eq. (C.12)

$$\alpha = -iR\sqrt{2\pi} \langle 0 | \eta^{(s), \frac{1}{2}, -\frac{1}{2}} | \chi^{\frac{1}{2}} \rangle. \quad (\text{C.23})$$

Hence,

$$\langle 0 | \chi_{(1/2)}(\mathbf{r}_1) \chi^{(1/2)}(\mathbf{r}_2) | 0 \rangle = R^{-2} \frac{\langle 0 | \eta_{(1/2)}(\mathbf{r}_1) \eta^{(1/2)}(\mathbf{r}_2) | 0 \rangle}{\frac{1}{2\pi} |\langle 0 | \eta^{(s), \frac{1}{2}, -\frac{1}{2}} | \chi^{\frac{1}{2}} \rangle|^2} \quad (\text{C.24})$$

and the dimensionless correlator Eq. (5.4) is exactly expressed as

$$C_\chi^*(\gamma_{12}) = \frac{\langle 0 | \eta_{(1/2)}(\mathbf{r}_1) \eta^{(1/2)}(\mathbf{r}_2) | 0 \rangle}{\frac{i}{\pi} |\langle 0 | \eta^{(s), \frac{1}{2}, -\frac{1}{2}} | \chi^{\frac{1}{2}} \rangle|^2}. \quad (\text{C.25})$$

Bibliography

- [1] A.M. Polyakov, *Conformal symmetry of critical fluctuations*, *JETP Lett.* **12** (1970) 381.
- [2] J.L. Cardy, *Scaling and Renormalization in Statistical Physics*, Cambridge Lecture Notes in Physics, Cambridge University Press (1996).
- [3] S. Sachdev, *Quantum Phase Transitions*, Cambridge University Press, 2 ed. (2011), [10.1017/CBO9780511973765](https://doi.org/10.1017/CBO9780511973765).
- [4] J. Polchinski, *String theory. Vol. 1: An introduction to the bosonic string*, Cambridge Monographs on Mathematical Physics, Cambridge University Press (12, 2007), [10.1017/CBO9780511816079](https://doi.org/10.1017/CBO9780511816079).

- [5] J.M. Maldacena, *The large- N limit of superconformal field theories and supergravity*, *Adv. Theor. Math. Phys.* **2** (1998) 231.
- [6] A.B. Zamolodchikov, *Irreversibility of the flux of the renormalization group in a 2D field theory*, *JETP Lett.* **43** (1986) 730.
- [7] P. Di Francesco, P. Mathieu and D. Sénéchal, *Conformal field theory*, Graduate texts in contemporary physics, Springer, New York, NY (1997), [10.1007/978-1-4612-2256-9](https://doi.org/10.1007/978-1-4612-2256-9).
- [8] P.H. Ginsparg, *Applied conformal field theory*, in *Les Houches Summer School in Theoretical Physics: Fields, Strings, Critical Phenomena*, 9, 1988 [[arXiv:hep-th/9108028](https://arxiv.org/abs/hep-th/9108028)].
- [9] A.A. Belavin, A.M. Polyakov and A.B. Zamolodchikov, *Infinite conformal symmetry in two-dimensional quantum field theory*, *Nucl. Phys. B* **241** (1984) 333.
- [10] D. Poland, S. Rychkov and A. Vichi, *The conformal bootstrap: Theory, numerical techniques, and applications*, *Rev. Mod. Phys.* **91** (2019) 015002 [[arXiv:1805.04405](https://arxiv.org/abs/1805.04405)].
- [11] S. Rychkov and N. Su, *New developments in the numerical conformal bootstrap*, *Rev. Mod. Phys.* **96** (2024) 045004 [[arXiv:2311.15844](https://arxiv.org/abs/2311.15844)].
- [12] T. Grover, D.N. Sheng and A. Vishwanath, *Emergent space-time supersymmetry at the boundary of a topological phase*, *Science* **344** (2014) 280 [[arXiv:1301.7449](https://arxiv.org/abs/1301.7449)].
- [13] J. Rong and N. Su, *Bootstrapping the minimal $\mathcal{N} = 1$ superconformal field theory in three dimensions*, *JHEP* **06** (2021) 154 [[arXiv:1807.04434](https://arxiv.org/abs/1807.04434)].
- [14] A. Atanasov, A. Hillman and D. Poland, *Bootstrapping the minimal 3d SCFT*, *JHEP* **11** (2018) 140 [[arXiv:1807.05702](https://arxiv.org/abs/1807.05702)].
- [15] D. Chowdhury, S. Raju, S. Sachdev, A. Singh and P. Strack, *Multipoint correlators of conformal field theories: implications for quantum critical transport*, *Phys. Rev. B* **87** (2013) 085138 [[arXiv:1210.5247](https://arxiv.org/abs/1210.5247)].
- [16] E. Katz, S. Sachdev, E.S. Sørensen and W. Witczak-Krempa, *Conformal field theories at nonzero temperature: Operator product expansions, Monte Carlo, and holography*, *Phys. Rev. B* **90** (2014) 245109 [[arXiv:1409.3841](https://arxiv.org/abs/1409.3841)].
- [17] J. Cai, E. Anderson, C. Wang, X. Zhang, X. Liu, W. Holtzmann et al., *Signatures of fractional quantum anomalous Hall states in twisted MoTe₂*, *Nature* **622** (2023) 63 [[arXiv:1809.09091](https://arxiv.org/abs/1809.09091)].
- [18] Y. Zeng, Z. Xia, K. Kang, J. Zhu, P. Knüppel, C. Vaswani et al., *Thermodynamic evidence of fractional Chern insulator in moiré MoTe₂*, *Nature* **622** (2023) 69 [[arXiv:2305.00973](https://arxiv.org/abs/2305.00973)].

[19] H. Park, J. Cai, E. Anderson, Y. Zhang, J. Zhu, X. Liu et al., *Observation of fractionally quantized anomalous hall effect*, *Nature* **622** (2023) 74 [arXiv:2308.02657].

[20] J.Y. Lee, C. Wang, M.P. Zaletel, A. Vishwanath and Y.-C. He, *Emergent multi-flavor QED₃ at the plateau transition between fractional Chern insulators: Applications to graphene heterostructures*, *Phys. Rev. X* **8** (2018) 031015 [arXiv:1802.09538].

[21] X.-Y. Song, Y.-H. Zhang and T. Senthil, *Phase transitions out of quantum Hall states in Moiré materials*, *Phys. Rev. B* **109** (2024) 085143 [arXiv:2308.10903].

[22] X.-Y. Song, C.-M. Jian, L. Fu and C. Xu, *Intertwined fractional quantum anomalous Hall states and charge density waves*, *Phys. Rev. B* **109** (2024) 115116 [arXiv:2310.11632].

[23] W. Zhu, C. Han, E. Huffman, J.S. Hofmann and Y.-C. He, *Uncovering conformal symmetry in the 3d Ising transition: State-operator correspondence from a quantum fuzzy sphere regularization*, *Phys. Rev. X* **13** (2023) 021009 [arXiv:2210.13482].

[24] L. Hu, Y.-C. He and W. Zhu, *Operator product expansion coefficients of the 3d Ising criticality via quantum fuzzy spheres*, *Phys. Rev. Lett.* **131** (2023) 031601 [arXiv:2303.08844].

[25] C. Han, L. Hu, W. Zhu and Y.-C. He, *Conformal four-point correlators of the three-dimensional Ising transition via the quantum fuzzy sphere*, *Phys. Rev. B* **108** (2023) 235123 [arXiv:2306.04681].

[26] Z. Zhou, L. Hu, W. Zhu and Y.-C. He, *SO(5) deconfined phase transition under the fuzzy-sphere microscope: Approximate conformal symmetry, pseudo-criticality, and operator spectrum*, *Phys. Rev. X* **14** (2024) 021044 [arXiv:2306.16435].

[27] L. Hu, Y.-C. He and W. Zhu, *Solving conformal defects in 3d conformal field theory using fuzzy sphere regularization*, *Nature Commun.* **15** (2024) 9013 [arXiv:2308.01903].

[28] J.S. Hofmann, F. Goth, W. Zhu, Y.-C. He and E. Huffman, *Quantum Monte Carlo simulation of the 3d Ising transition on the fuzzy sphere*, *SciPost Phys. Core* **7** (2024) 028 [arXiv:2310.19880].

[29] C. Han, L. Hu and W. Zhu, *Conformal operator content of the Wilson-Fisher transition on fuzzy sphere bilayers*, *Phys. Rev. B* **110** (2024) 115113 [arXiv:2312.04047].

[30] Z. Zhou, D. Gaiotto, Y.-C. He and Y. Zou, *The g-function and defect changing operators from wavefunction overlap on a fuzzy sphere*, *SciPost Phys.* **17** (2024) 021 [arXiv:2401.00039].

- [31] L. Hu, W. Zhu and Y.-C. He, *Entropic F -function of 3d Ising conformal field theory via the fuzzy sphere regularization*, *Phys. Rev. B* **111** (2025) 155151 [[arXiv:2401.17362](https://arxiv.org/abs/2401.17362)].
- [32] G. Cuomo, Y.-C. He and Z. Komargodski, *Impurities with a cusp: general theory and 3d Ising*, *JHEP* **11** (2024) 061 [[arXiv:2406.10186](https://arxiv.org/abs/2406.10186)].
- [33] Z. Zhou and Y. Zou, *Studying the 3d Ising surface CFTs on the fuzzy sphere*, *SciPost Phys.* **18** (2025) 031 [[arXiv:2407.15914](https://arxiv.org/abs/2407.15914)].
- [34] B.-B. Chen, X. Zhang and Z. Yang Meng, *Emergent conformal symmetry at the multicritical point of $(2+1)d$ SO(5) model with Wess-Zumino-Witten term on a sphere*, *Phys. Rev. B* **110** (2024) 125153 [[arXiv:2405.04470](https://arxiv.org/abs/2405.04470)].
- [35] M. Dedushenko, *Ising BCFT from fuzzy hemisphere*, [arXiv:2407.15948](https://arxiv.org/abs/2407.15948).
- [36] G. Fardelli, A.L. Fitzpatrick and E. Katz, *Constructing the infrared conformal generators on the fuzzy sphere*, *SciPost Phys.* **18** (2025) 086 [[arXiv:2409.02998](https://arxiv.org/abs/2409.02998)].
- [37] R. Fan, *Note on explicit construction of conformal generators on the fuzzy sphere*, [arXiv:2409.08257](https://arxiv.org/abs/2409.08257).
- [38] Z. Zhou and Y.-C. He, *3d conformal field theories with $Sp(N)$ global symmetry on a fuzzy sphere*, *Phys. Rev. Lett.* **135** (2025) 026504 [[arXiv:2410.00087](https://arxiv.org/abs/2410.00087)].
- [39] C. Voinea, R. Fan, N. Regnault and Z. Papić, *Regularizing 3d conformal field theories via anyons on the fuzzy sphere*, *Phys. Rev. X* **15** (2025) 031007 [[arXiv:2411.15299](https://arxiv.org/abs/2411.15299)].
- [40] S. Yang, Y.-G. Yue, Y. Tang, C. Han, W. Zhu and Y. Chen, *Microscopic study of the three-dimensional Potts phase transition via fuzzy sphere regularization*, *Phys. Rev. B* **112** (2025) 024436 [[arXiv:2501.14320](https://arxiv.org/abs/2501.14320)].
- [41] C. Han and W. Zhu, *Quantum phase transitions on the noncommutative circle*, *Phys. Rev. B* **111** (2025) 085113.
- [42] A.M. Läuchli, L. Herviou, P.H. Wilhelm and S. Rychkov, *Exact diagonalization, matrix product states and conformal perturbation theory study of a 3d Ising fuzzy sphere model*, [arXiv:2504.00842](https://arxiv.org/abs/2504.00842).
- [43] R. Fan, J. Dong and A. Vishwanath, *Simulating the non-unitary Yang-Lee conformal field theory on the fuzzy sphere*, [arXiv:2505.06342](https://arxiv.org/abs/2505.06342).
- [44] E. Arguello Cruz, I.R. Klebanov, G. Tarnopolsky and Y. Xin, *Yang-Lee quantum criticality in various dimensions*, [arXiv:2505.06369](https://arxiv.org/abs/2505.06369).

[45] J. Elias Miró and O. Delouche, *Flowing from the Ising model on the fuzzy sphere to the 3d Lee-Yang CFT*, [arXiv:2505.07655](https://arxiv.org/abs/2505.07655).

[46] Y.-C. He, *Free real scalar CFT on fuzzy sphere: spectrum, algebra and wavefunction ansatz*, [arXiv:2506.14904](https://arxiv.org/abs/2506.14904).

[47] J. Taylor, C. Voinea, Z. Papić and R. Fan, *Conformal scalar field theory from Ising tricriticality on the fuzzy sphere*, [arXiv:2506.22539](https://arxiv.org/abs/2506.22539).

[48] S. Yang, L.-D. Hu, C. Han, W. Zhu and Y. Chen, *Conformal operator flows of the deconfined quantum criticality from $SO(5)$ to $O(4)$* , [arXiv:2507.01322](https://arxiv.org/abs/2507.01322).

[49] Z. Zhou, C. Wang and Y.-C. He, *Chern-Simons-matter conformal field theory on fuzzy sphere: Confinement transition of Kalmeyer-Laughlin chiral spin liquid*, [arXiv:2507.19580](https://arxiv.org/abs/2507.19580).

[50] J.-M. Dong, Y. Zhang, K.-W. Huang, H.-H. Tu and Y.-H. Wu, *Numerical extraction of crosscap coefficients in microscopic models for $(2+1)D$ conformal field theory*, [arXiv:2507.20005](https://arxiv.org/abs/2507.20005).

[51] Z.-Q. Gao, T. Wang and D.-H. Lee, *Interacting chern insulator transition on the sphere: revealing the Gross-Neveu-Yukawa criticality*, [arXiv:2504.15338](https://arxiv.org/abs/2504.15338).

[52] N. Read and D. Green, *Paired states of fermions in two-dimensions with breaking of parity and time reversal symmetries, and the fractional quantum Hall effect*, *Phys. Rev. B* **61** (2000) 10267 [[arXiv:cond-mat/9906453](https://arxiv.org/abs/cond-mat/9906453)].

[53] X.L. Qi and S.C. Zhang, *Topological insulators and superconductors*, *Rev. Mod. Phys.* **83** (2011) 1057 [[arXiv:1008.2026](https://arxiv.org/abs/1008.2026)].

[54] G.W. Moore and N. Read, *Nonabelions in the fractional quantum Hall effect*, *Nucl. Phys. B* **360** (1991) 362.

[55] E.H. Fradkin and S.H. Shenker, *Phase Diagrams of Lattice Gauge Theories with Higgs Fields*, *Phys. Rev. D* **19** (1979) 3682.

[56] J.B. Kogut, *An isntruction to lattice gauge theory and spin systems*, *Rev. Mod. Phys.* **51** (1979) 659.

[57] R.A. Jalabert and S. Sachdev, *Spontaneous alignment of frustrated bonds in an anisotropic, three-dimensional Ising model*, *Phys. Rev. B* **44** (1991) 686.

[58] S. Sachdev and J. Ye, *Universal quantum critical dynamics of two-dimensional antiferromagnets*, *Phys. Rev. Lett.* **69** (1992) 2411 [[arXiv:cond-mat/9204001](https://arxiv.org/abs/cond-mat/9204001)].

[59] T. Senthil and M.P.A. Fisher, *z_2 gauge theory of electron fractionalization in strongly correlated systems*, *Phys. Rev. B* **62** (2000) 7850 [[arXiv:cond-mat/9910224](https://arxiv.org/abs/cond-mat/9910224)].

[60] S. Sachdev and M. Vojta, *Translational symmetry breaking in two-dimensional antiferromagnets and superconductors*, *J. Phys. Soc. Jpn. Suppl. B* **69** (2021) [[arXiv:cond-mat/9910231](https://arxiv.org/abs/cond-mat/9910231)].

[61] M. Schuler, S. Whitsitt, L.-P. Henry, S. Sachdev and A.M. Läuchli, *Universal signatures of quantum critical points from finite-size torus spectra: A window into the operator content of higher-dimensional conformal field theories*, *Phys. Rev. Lett.* **117** (2016) 210401 [[arXiv:1603.03042](https://arxiv.org/abs/1603.03042)].

[62] E. Witten, *Three-dimensional gravity revisited*, [arXiv:0706.3359](https://arxiv.org/abs/0706.3359).

[63] A. Maloney and E. Witten, *Quantum gravity partition functions in three dimensions*, *JHEP* **02** (2010) 029 [[arXiv:0712.0155](https://arxiv.org/abs/0712.0155)].

[64] L.F. Alday and S.M. Chester, *Pure anti-de Sitter supergravity and the conformal bootstrap*, *Phys. Rev. Lett.* **129** (2022) 211601 [[arXiv:2207.05085](https://arxiv.org/abs/2207.05085)].

[65] J. Gomis, Z. Komargodski and N. Seiberg, *Phases of adjoint QCD_3 and dualities*, *SciPost Phys.* **5** (2018) 007 [[arXiv:1710.03258](https://arxiv.org/abs/1710.03258)].

[66] J. Madore, *The fuzzy sphere*, *Class. Quant. Grav.* **9** (1992) 69.

[67] F.D.M. Haldane, *Fractional quantization of the Hall effect: A hierarchy of incompressible quantum fluid states*, *Phys. Rev. Lett.* **51** (1983) 605.

[68] T.T. Wu and C.N. Yang, *Dirac monopole without strings: Monopole harmonics*, *Nucl. Phys. B* **107** (1976) 365.

[69] N. Regnault and T. Jolicoeur, *Quantum Hall fractions for spinless bosons*, *Phys. Rev. B* **69** (2004) 235309 [[arXiv:cond-mat/0312248](https://arxiv.org/abs/cond-mat/0312248)].

[70] X.G. Wen and A. Zee, *Shift and spin vector: New topological quantum numbers for the Hall fluids*, *Phys. Rev. Lett.* **69** (1992) 953.

[71] X.G. Wen and A. Zee, *A classification of Abelian quantum Hall states and matrix formulation of topological fluids*, *Phys. Rev. B* **46** (1992) 2290.

[72] Z. Zhou, *Fuzzified : Julia package for numerics on the fuzzy sphere*, [arXiv:2503.00100](https://arxiv.org/abs/2503.00100).

[73] J. Dubail, N. Read and E.H. Rezayi, *Real-space entanglement spectrum of quantum Hall systems*, *Phys. Rev. B* **85** (2012) 115321 [[arXiv:1111.2811](https://arxiv.org/abs/1111.2811)].

[74] A. Sterdyniak, A. Chandran, N. Regnault, B.A. Bernevig and P. Bonderson, *Real-space entanglement spectrum of quantum Hall states*, *Phys. Rev. B* **85** (2012) 125308 [[arXiv:1110.2810](https://arxiv.org/abs/1110.2810)].

[75] H. Li and F. Haldane, *Entanglement spectrum as a generalization of entanglement entropy: Identification of topological order in non-Abelian fractional quantum Hall effect states*, *Phys. Rev. Lett.* **101** (2008) 010504 [[arXiv:0805.0332](https://arxiv.org/abs/0805.0332)].

[76] A. Kitaev, *Anyons in an exactly solved model and beyond*, *Annals Phys.* **321** (2006) 2 [[arXiv:cond-mat/0506438](https://arxiv.org/abs/cond-mat/0506438)].

[77] P.-S. Hsin and N. Seiberg, *Level/rank duality and Chern-Simons-matter theories*, *JHEP* **09** (2016) 095 [[arXiv:1607.07457](https://arxiv.org/abs/1607.07457)].

[78] O. Aharony, F. Benini, P.-S. Hsin and N. Seiberg, *Chern-Simons-matter dualities with SO and USp gauge groups*, *JHEP* **02** (2017) 072 [[arXiv:1611.07874](https://arxiv.org/abs/1611.07874)].

[79] C. Cordova, P.-S. Hsin and N. Seiberg, *Global symmetries, counterterms, and duality in Chern-Simons matter theories with orthogonal gauge groups*, *SciPost Phys.* **4** (2018) 021 [[arXiv:1711.10008](https://arxiv.org/abs/1711.10008)].

[80] J.L. Cardy, *Boundary conditions, fusion rules and the verlinde formula*, *Nucl. Phys. B* **324** (1989) 581.

[81] M. Oshikawa and I. Affleck, *Boundary conformal field theory approach to the critical two-dimensional ising model with a defect line*, *Nucl. Phys. B* **495** (1997) 533 [[arXiv:cond-mat/9612187](https://arxiv.org/abs/cond-mat/9612187)].

[82] R.A. Lanzetta, S. Liu and M.A. Metlitski, *The beginning of the endpoint bootstrap for conformal line defects*, [arXiv:2508.14964](https://arxiv.org/abs/2508.14964).

[83] Y. Zou, *Universal information of critical quantum spin chains from wavefunction overlap*, *Phys. Rev. B* **105** (2022) 165420 [[arXiv:2104.00103](https://arxiv.org/abs/2104.00103)].

[84] Y. Liu, Y. Zou and S. Ryu, *Operator fusion from wave-function overlap: Universal finite-size corrections and application to the Haagerup model*, *Phys. Rev. B* **107** (2023) 155124 [[arXiv:2203.14992](https://arxiv.org/abs/2203.14992)].

[85] S.M. Chester, L.V. Iliesiu, M. Mezei and S.S. Pufu, *Monopole operators in U(1) Chern-Simons-matter theories*, *JHEP* **05** (2018) 157 [[arXiv:1710.00654](https://arxiv.org/abs/1710.00654)].

[86] E. Witten, *Supersymmetric index of three-dimensional gauge theory*, [arXiv:hep-th/9903005](https://arxiv.org/abs/hep-th/9903005).

[87] J.K. Jain, *Composite fermion approach for the fractional quantum Hall effect*, *Phys. Rev. Lett.* **63** (1989) 199.

[88] R.B. Laughlin, *Anomalous quantum Hall effect: An incompressible quantum fluid with fractionally charged excitations*, *Phys. Rev. Lett.* **50** (1983) 1395.

[89] N. Read and E. Rezayi, *Beyond paired quantum Hall states: Parafermions and incompressible states in the first excited Landau level*, *Phys. Rev. B* **59** (1999) 8084 [[arXiv:cond-mat/9809384](https://arxiv.org/abs/cond-mat/9809384)].

[90] M. Billó, M. Caselle, D. Gaiotto, F. Gliozzi, M. Meineri and R. Pellegrini, *Line defects in the 3d Ising model*, *JHEP* **07** (2013) 055 [[arXiv:1304.4110](https://arxiv.org/abs/1304.4110)].

[91] C. Töke, N. Regnault and J.K. Jain, *Nature of excitations of the 5/2 fractional quantum Hall effect*, *Phys. Rev. Lett.* **98** (2007) [[arXiv:cond-mat/0609177](https://arxiv.org/abs/cond-mat/0609177)].

[92] I.S. Tupitsyn, A. Kitaev, N.V. Prokof'ev and P.C.E. Stamp, *Topological multicritical point in the toric code and 3d gauge Higgs models*, *Phys. Rev. B* **82** (2010) 085114 [[arXiv:0804.3175](https://arxiv.org/abs/0804.3175)].

[93] A.M. Somoza, P. Serna and A. Nahum, *Self-dual criticality in three-dimensional \mathbb{Z}_2 gauge theory with matter*, *Phys. Rev. X* **11** (2021) 041008 [[arXiv:2012.15845](https://arxiv.org/abs/2012.15845)].

[94] Y. Barlas and K. Yang, *Fractionalization via \mathbb{Z}_2 gauge fields at a cold atom quantum Hall transition*, *Phys. Rev. Lett.* **106** (2011) 170403 [[arXiv:1012.0046](https://arxiv.org/abs/1012.0046)].

[95] S.-F. Liou, Z.-X. Hu and K. Yang, *Topological quantum phase transition from a fermionic integer quantum Hall phase to a bosonic fractional quantum Hall phase through a p-wave Feshbach resonance*, *Phys. Rev. B* **95** (2017) 241106 [[arXiv:1704.05035](https://arxiv.org/abs/1704.05035)].

[96] C. Voinea, W. Zhu, N. Regnault, and Z. Papic, *Critical majorana fermion at a topological quantum Hall bilayer transition*, (to appear) .